

Synthesis of Cantharidin Derivatives as Photo-Initiated DNA Cleavage Agents

Wu CY¹, Lin PY², Yu SSF³, Chu PC^{4,5} and Su CJ^{1,6*}

¹School of Medical Applied Chemistry, Chung Shan Medical University, Taiwan (R.O.C.)

²School of Pharmacy, Taipei Medical University, Taiwan (R.O.C.)

³Institute of Chemistry, Academia Sinica, Taiwan (R.O.C.)

⁴Department of Environmental and Occupational Medicine, National Taiwan University College of Medicine, Taiwan (R.O.C.)

⁵Department of Environmental and Occupational Medicine, National Taiwan University Hospital, Taiwan (R.O.C.)

⁶Department of Medical Research, Chung Shan Medical University Hospital, Taiwan (R.O.C.)

***Corresponding author:** Chi Jung Su, School of Medical Applied Chemistry, Chung Shan Medical University, No. 110, Sec. 1, Jianguo N. Rd, South Dist., Taichung 40201, Taiwan (R.O.C.), Tel: +886-4-24730022, +886-921-785-188; Email: sucj514@gmail.com

Volume 3 Issue 3

Received Date: September 11, 2019

Published Date: October 15, 2019

DOI: 10.23880/macij-16000146

Published by



MEDWIN PUBLISHERS

Committed to Create Value for Researchers

Table of Contents

Abstract	1
Introduction	2
Cantharidin	2
Other Chemical Materials	3
Deoxyribonucleic Acid (DNA)	4
DNA Damage	5
Types of DNA Damage	6
Correlative Analysis Methods	8
Motive	10
Materials and Methods	10
Extract Cantharidin from Beetles (Table 3)	10
Synthesis (Table 4)	10
The Growth of <i>Escherichia coli</i> (pUC19 DH5 α) (Table 5)	11
Purification Plasmid DNA (Table 6)	12
Photoreaction & DNA Cleavage Studies via Supercoiled Plasmid (Table 7 & 8)	12
Explore the DNA Cleavage with Site Specificity (Table 9)	14
Results and Discussion	16
Synthesis	16
Prepare Super-Coiled DNA	20
DNA Cleavage Studies Mediated by Cantharidin Derivatives Using Supercoiled Plasmid pUC19	21
Explore the DNA Cleavage with Site Specificity	25
Conclusion	26
References	26

Abstract

Previous studies indicated that cantharidin (exo-2,3-dimethyl-7-oxabicyclo [2,2,1] heptane-2,3-dicarboxylic anhydride) could inhibit the proliferation of cancer cells via p53 dependent mechanism. It could also inhibit protein phosphatases 1 (PP1) and protein phosphatases 2A (PP2A). When cantharidin was treated with cancer cell, it could induce to produce oxidative stress. Oxidative stress would cause damage the single and double stand DNA increasingly. But the mechanism of anticancer is still not clear. Here, cantharidin and cantharidin derivatives were served as photo-initiated DNA cleavage agents. We combined them with irradiation ($\lambda=352\text{nm}$) to see if they have the ability to cleavage the supercoiled DNA. The results displayed that the cantharidin derivatives could cleavage DNA at acidic condition with irradiation. Then, we used high-resolution gel electrophoresis to analyze the results and the experiment of Maxam-Gilbert was served as standard. The results indicated that cantharidin derivatives have better ability of cleavage at the guanine site.

Keywords: DNA Cleavage Agents; Cantharidin Derivatives; Diels-Alder Reaction

Abbreviations: PP1: Protein Phosphatases 1; PP2A: Protein Phosphatases 2A; ROS: Reactive Oxygen Species; DNA: Deoxyribonucleic Acid; SAM: S-Adenosyl Methionine; APS: Ammonium Per Sulfate.

Introduction

Cantharidin

Cantharidin, a traditional Chinese medicine, is a poisonous chemical compound secreted by many species of blister beetle, and the most notable one is secreted by the Spanish fly, *Mylabris phalerata* Pall or *M. cichorii* L. The false blister beetles and cardinal beetles also have cantharidin. It was first isolated by Pierre Robiquent in 1810. Dadamen confirmed the structure of cantharidin in 1914. Cantharidin is also called *exo*, *exo*-2,3-dimethyl-7-oxobicyclo [2.2.1] heptane-2,3-dicarboxylic acid anhydride (Figures 1.1 & 1.2) and secreted by the male blister beetle which will be given to the female during the mating. Afterwards the female beetle will cover its eggs with it as a defense against predators. Researchers of Harvard University, such as Woodward R B, et al. they synthesize desoxycanthalidone in 1941 [1]. A total synthesis of cantharidin (I) from the butadiene adduct (X) of dimethyl 3,6-epoxy-3,4,5,6-tetrahydrophthalate (IX) was described by Stork G, et al. [2,3]. Efficient total synthesis of Cantharidin via a High-Pressure Diels-Alder Reaction was carried out by Dauben W. G. and Krabbenhoft H O [4,5]. We use the method which is developed by Lin P. Y. in our laboratory because High-Pressure Diels-Alder Reaction is too dangerous. We use dried bodies of those beetles to extract cantharidin (Scheme 1) [6].



Figure 1.1: The dried bodies of *Mylabris phalerata* Pall.

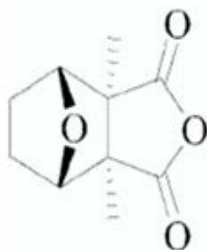
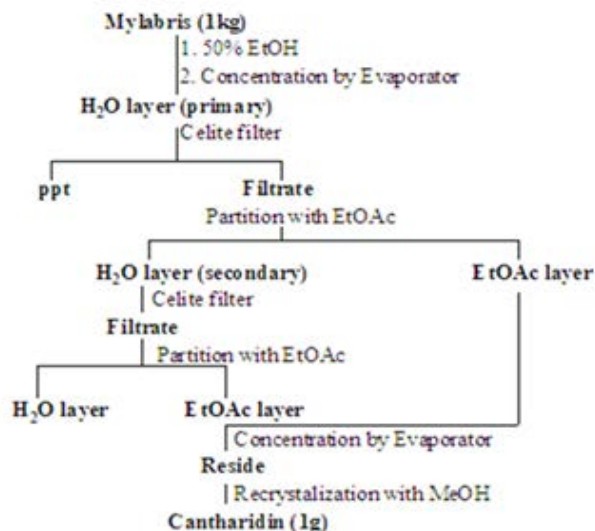


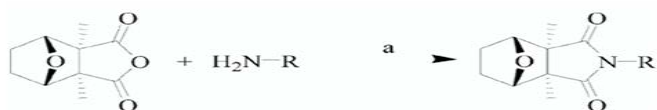
Figure 1.2: Structure of cantharidin.



Scheme 1: Preparation of cantharidin.

Cantharidin has been reported to be active which can inhibit cancer cell proliferation in 1264. Recently, some reports indicate cantharidin and cantharidin derivatives have clinical potential, which can be seen as protein phosphatase 1 (PP1) and protein phosphatase 2A (PP2A) inhibitors [7]. This activity is necessary for the growth inhibition activity of these compounds. Protein phosphatases are involved, among others, in the regulation of multiple cellular processes including signal transduction pathway, cell cycle progression, glucose metabolism, and calcium transport [8]. Cantharidin can also induce leukemia cell apoptosis by p53-dependent mechanism [9]. A previous study suggested that treatment with several analogs of cantharidin increase the activity of xanthine oxidase which would result in an increased production of reactive oxygen species (ROS) [10]. ROS are well known as DNA damaging agents [11]. Via comet assay, DNA single- and double-strands can be broken by treating cantharidin. Thus, although the biochemical target of cantharidin and its derivative is known, but the critical molecular pathways about how cantharidin and its derivative cause growth inhibition of cell death are unclear.

Cantharidin Derivatives: Cantharidin has been reported to be active against various human cancers, especially hepatocarcinoma; however, its severe renal toxicity limits the development as chemotherapeutic agents [12,13]. Lin P Y, et al. synthesized a series of novel cantharidinimides and cantharidin derivatives by using high pressure and evaluated their cytotoxicities against human carcinoma cells [14,15] (Scheme 2).



Scheme 2: Synthesis of novel cantharidinimides by using high pressure.¹⁴ (a): TEA, Toluene, c.a. 200°C reflux, R = Amines.

Other Chemical Materials

Many mutagens fit into the space between DNA two adjacent base pairs of DNA, this is called intercalating. Most intercalators are aromatic and planar molecules. In order for an intercalator to fit between base pairs, the bases must be separated and distorted the DNA strands by unwinding of the double helix. This inhibits both transcription and DNA replication, causing toxicity and mutations. As a result, DNA intercalators are often carcinogens. Acridines, aflatoxin and ethidium bromide are well-known examples [16-18] (Figures 1.3-1.7).

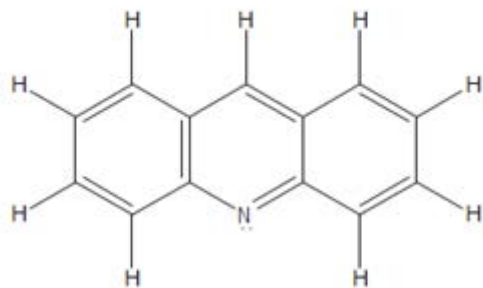


Figure 1.3: Structure of Acridines.

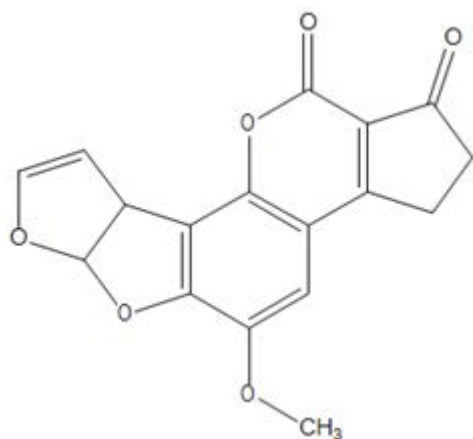


Figure 1.4: Structure of aflatoxin.

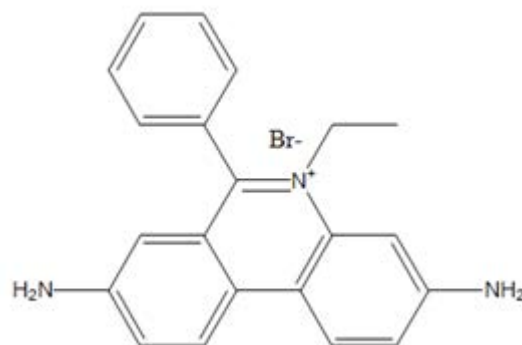


Figure 1.5: Structure of ethidium bromide.

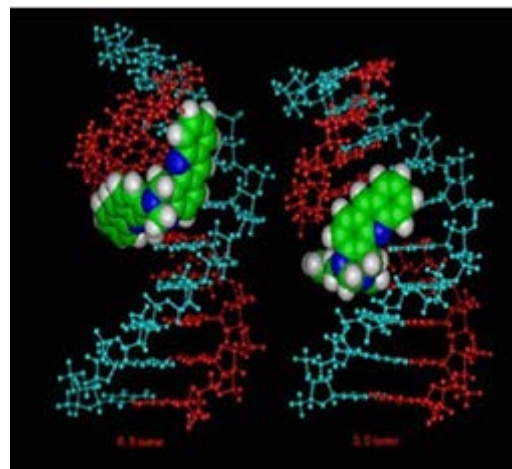


Figure 1.6: Structure of acridines intercalate with DNA [19].

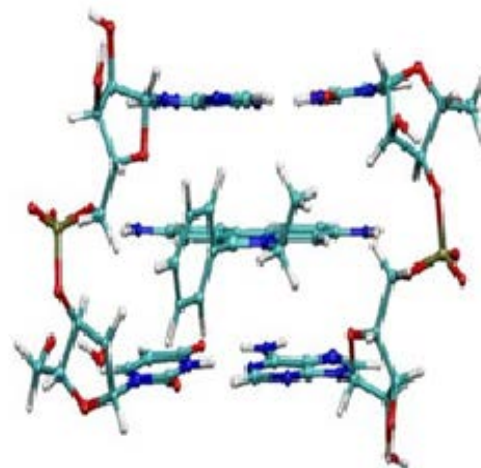


Figure 1.7: Structure of ethidium bromide intercalate with DNA [20].

Deoxyribonucleic Acid (DNA)

Deoxyribonucleic acid (DNA) is nucleic acid that contains the genetic instructions used in the development and functioning of all known living organisms and some viruses. The main role of DNA molecules is the long-term storage of information. It stores the genetic messages to lead with the features of the life such as replication, metabolism and physiological processes of bio-organisms. Of course, to facilitate the construction of other components of cells, such as proteins and RNA molecules are also guided by the genetic codes of DNA. DNA is a long polymer made from repeating units which called nucleotides [21]. The DNA chain ranges from 22 to 26 Angstroms wide (2.2 to 2.6 nanometers), and one nucleotide unit is 3.3 Å (0.33 nm) long.

In living organisms, DNA does not usually exist as a single molecule, but instead as a tightly-associated pair of molecules [22]. These two long strands entwine like vine, in the shape of a double helix. The nucleotide repeats contain both the segment of the backbone of the molecule, which holds the chain together, and a base linked to a sugar is called a sugar and one or more phosphate groups is called a nucleotide. If many nucleotides are linked together, as in DNA, the nomenclature of the corresponding polymer is a

polynucleotide [23].

The backbone of DNA strand is made from alternating phosphate and sugar residues [24]. The sugar in DNA is 2-deoxyribose which is a pentose (five-carbon) sugar. The deoxyribose contains seven hydrogen atoms attached to the 5-membered ring, and generally designated these atoms as H-5', H-5'', H-4', H-3', H-2', H-2'', and H-1' (Figure 1.8) [25]. The sugar is joined together by phosphate groups derived from phosphodiester bonds between the third and fifth carbon atoms of adjacent sugar rings. The sugar-phosphate backbone is highly vulnerable to be attacked by free radical. Abstraction of a hydrogen atom from deoxyribose produces a carbon-based sugar radical that can rearrange, and culminate in scission of the nucleic acid strand [26]. Those asymmetric bonds mean a strand of DNA as a direction. In a double helix the direction of the nucleotide in one strand is opposite to their direction in the other strand. This arrangement of DNA strands is called anti-parallel. The asymmetric ends of DNA strands are referred to as the 5' (five prime) and 3' (three prime) ends. The 5' end is with a terminal phosphate group and the 3' end is with a terminal hydroxyl group (Figure 1.9). One of the major differences between DNA and RNA is sugar, 2-deoxyribose is replaced by the alternative pentose sugar ribose in RNA [27].

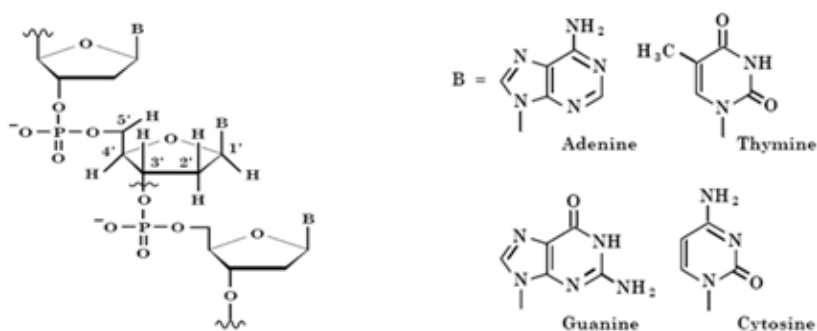


Figure 1.8: The seven deoxyribose hydrogen atoms and four bases.

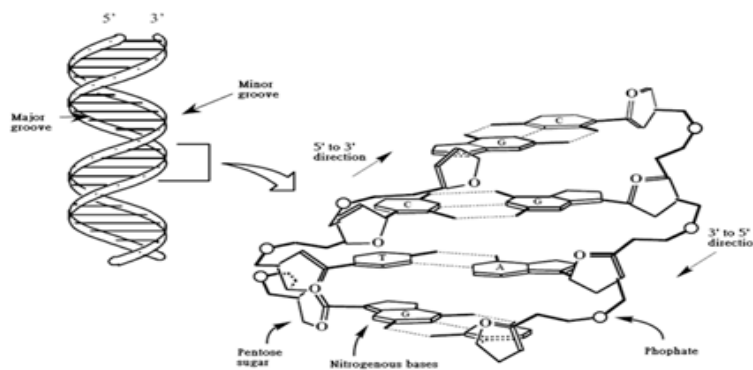


Figure 1.9: The structure of B from DNA.

The DNA double helix is stabilized by hydrogen bonds between the bases attached to the two strands. These bases are classified into two types; adenine (A) and guanine (G) are fused five- and six-membered heterocyclic compounds called purines, whereas cytosine (C) and thymine (T) are six-membered rings called pyrimidines (Figure 8). Another fifth pyrimidine base, called uracil (U), usually takes place of thymine in RNA and differs from thymine by lacking a methyl group on its ring. Uracil is not usually found in DNA, occurring only as a breakdown product of cytosine. Those four bases (A, T, C, and G) are attached to the sugar/phosphate to form the complete nucleotide, and each type of bases on one strand forms hydrogen bonding with just another specific type of base on the other strand. Here, purines form hydrogen bonds to pyrimidines, where A bonding only to T with two hydrogen bonds, and C bonding only to G with three hydrogen bonds.

This arrangement of two nucleotides binding together across the double helix is called base pair. As a result of this complement, all the information in the double-stranded sequence of a DNA helix is duplicated on each strand, which is vital in DNA replication. Indeed, this reversible and specific interaction between complementary base pair is critical for all the functions of DNA in living organisms [28]. Purine and pyrimidine heterocycles containing rich electrons are prime targets for reaction with electrophiles: alkylating agents, oxidizing agents and halogens. These reagents rarely lead to direct (or frank) strand scission, but allow DNA or RNA cleavage to arise site specifically in second chemical step, usually including heat, base, or enzyme treatment to effect deglycosylation and β -elimination of the 3'-phosphate (Figure 1.10) [29].

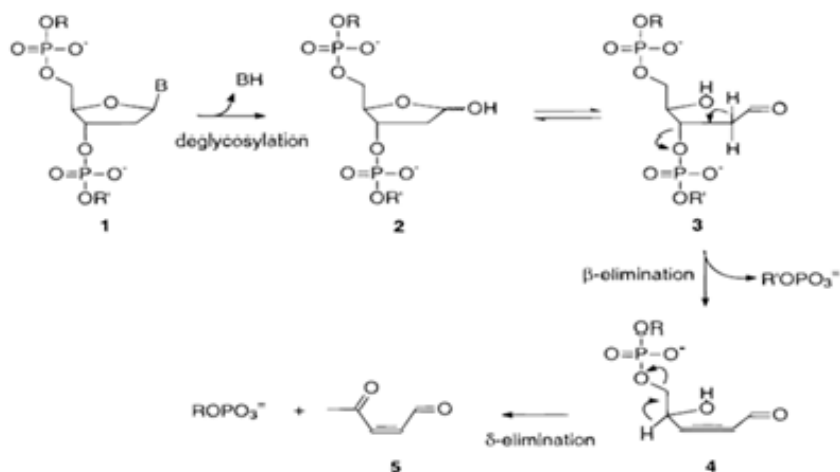


Figure 1.10: Mechanism of β -elimination and δ -elimination after formation of an abasic site.

Normally, the double helix is right-handed spiral. As the DNA strands wind around each other, they leave gaps between each set of phosphate backbones to combine bases inside together. There are two of these grooves twisting around the surface of the double helix: one groove is 22 Å wide and the other, the minor groove, is 12 Å wide [30]. The narrowness of the minor groove means that the edges of the bases are more accessible than the major groove. As a result, proteins like transcription factors can bind to specific sequences in double-stranded DNA which usually make contacts to the sides of the bases exposed in the major groove [31]. This situation varies in unusual conformations of DNA within the cell, but the major and minor grooves are always named to reflect the differences in size that would be seen if the DNA is twisted back into the ordinary B form.

DNA Damage

Sources of DNA damage can be sub-divided into endogenous damage and exogenous damage. DNA endogenous damage such as attacked by reactive oxygen species produced from normal metabolic byproducts (spontaneous mutation) can cause oxidation and deamination. Exogenous damage caused by external agents such as ultraviolet radiation from the sun, other radiation frequencies (x-rays and gamma rays), hydrolysis or thermal disruption, certain plant toxins and artificial mutagenic chemicals etc. Artificial mutagenic chemicals are able to cause DNA damage such as deoxyribose decomposed or nucleobase site oxidation. Furthermore, artificial mutagenic chemicals can cooperate with DNA discrimination systems to cleavage specific base site and hydrolyse phosphodiester

bond to form direct strand scission via irradiation, redox reaction or pH regulation. According to the conception of antisense genes, a single strand of DNA or RNA is purposely designed to prevent some translation from injurious proteins and artificial mutagenic chemicals which reveal the potential for the molecular engineering of DNA for genetic manipulation and gene therapy in biomedicine [32].

Types of DNA Damage

For DNA damages, there are four major types are corresponded to the base lesion and listed as follow:

Oxidation: Reactive oxygen species can cause base oxidation and interrupt DNA strand. Reactive oxygen species, such as hydroxyl radical, can be produced in various ways (Figure 1.11). Hydroxyl radical tends to attack guanine nucleobase. There are three major intermediates that result from hydroxyl radical oxidizing a guanine. These effects cause the formation of C4 adduct (1), C5 adduct (2), and the C8 adduct (3) (Figure 1.12).

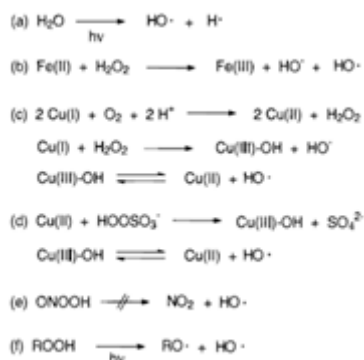


Figure 1.11: Reactions generating hydroxyl radical.

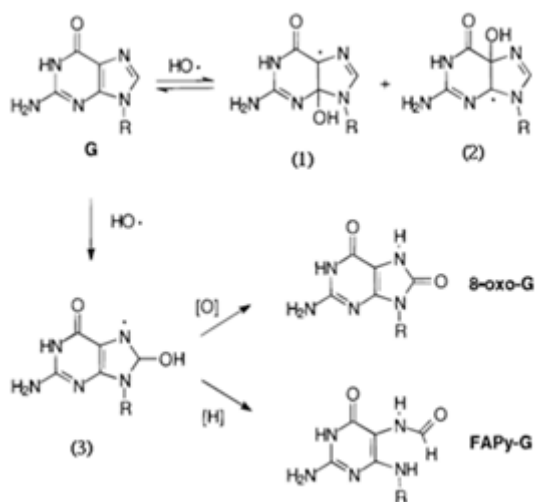


Figure 1.12: Addition of hydroxyl radical to guanine.

Alkylation: Methylation is the most common type of alkylation. DNA methylation typically occurs at CpG sites (cytosine-phosphate-guanine sites; where a cytosine is directly followed by guanine in DNA sequence); this methylation results in the conversion of the cytosine to 5-methylcytosine (Figure 1.13&1.14).

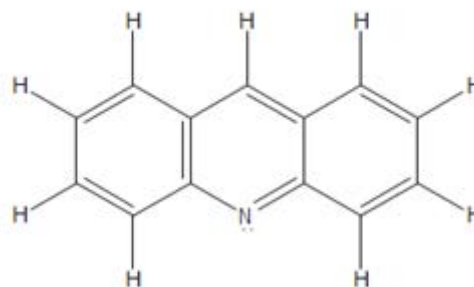


Figure 1.13: Mechanism of DNA methylation. 5-Methylcytosine is produced by action of the DNA methyltransferases which catalyse the transfer of methyl group (CH_3) from S-adenosylmethionine (SAM) to the carbon-5 position of cytosine.

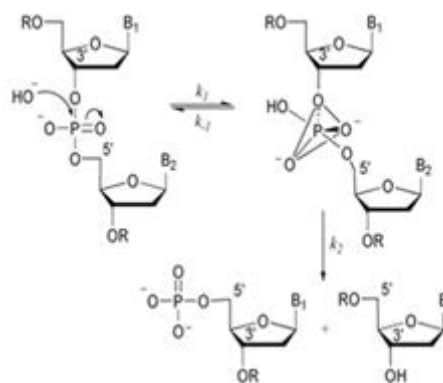


Figure 1.14: Reaction pathway for DNA hydrolysis. The enzymatically (DNMT) promoted P-O3' scission is shown.

Hydrolysis: Depurination or depyrimidination are DNA alteration in which the hydrolysis of the β -N-glycosidic link between purine or pyrimidine base and yield the deoxyribose-phosphate backbone [33].

Deamination: Spontaneous deamination is the hydrolysis reaction of cytosine into uracil which can release ammonia during the process. Deamination of 5-methylcytosine results in thymine and ammonia. This is the most common single nucleotide mutation and if it does not affect the function of the gene, the mutation will persist. Deamination of guanine results in the formation xanthine and producing hypoxanthine in adenine (Figure 1.15).

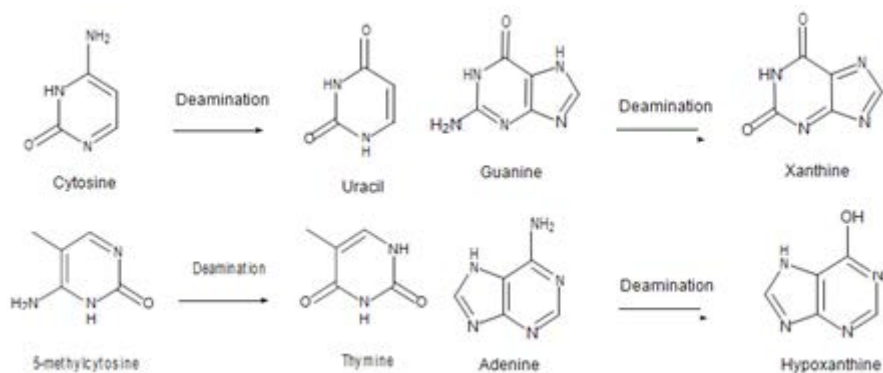


Figure 1.15: Examples of deamination which involves of an amino group.

Another DNA damage type is C-H abstraction on sugar moiety. For example, Rhodium (III) complex's (Figure 1.16) is a metal complexes that has been established to cleave DNA through abstraction of 3'-hydrogen. Rhodium (III) coordinated by well-known intercalating ligands is able to

bind to duplex DNA and generate strand breaks in presence. Previous studies revealed the products of this reaction to be, as shown in scheme 3. 5'-phosphate-terminated DNA strands, a DNA strand terminating in a 3'-phosphoglycaldehyde group and base propenoic acid.

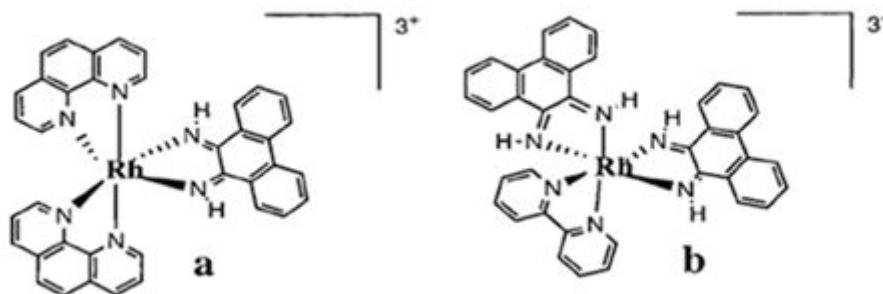
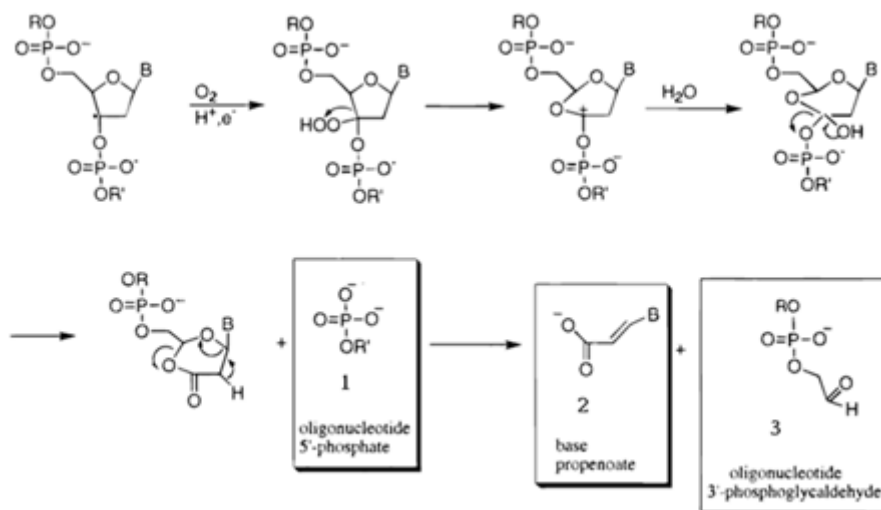


Figure 1.16: $[\text{Rh}(\text{phen})_2(\text{phi})]^{3+}$ (a) and $[\text{Rh}(\text{phi})_2(\text{bpy})]^{3+}$ (b).



Scheme 3: Proposed H-3C-Abstraction Pathway for DNA Strand Scission Mediated by $[\text{Rh}(\text{phen})_2(\text{phi})]^{3+}$ or $[\text{Rh}(\text{phi})_2(\text{bpy})]^{3+}$ under Aerobic Conditions (adapted from Sitlani et al. [34])

Correlative Analysis Methods

Scientists have used different techniques such as HPLC, PAGE or reaction with thiobarbituric acid to detect DNA damage products (Table 1). Gel electrophoresis is

employed to identify DNA strands lesion and Maxam-Gilbert sequencing reaction is used to determine DNA sequence. Recently, MALDI-TOF provides rapid and sensitive method to directly analyze not only site specificity but also DNA cleavage products [35].

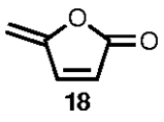
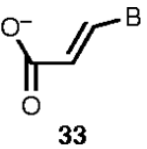
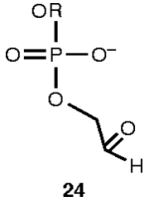
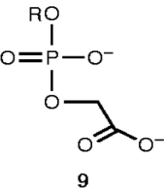
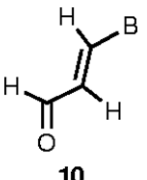
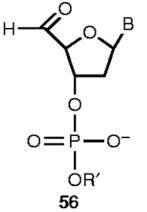
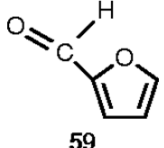
Marker Product		Position of Hydrogen abs Traction	How Detected
 18	5-methylene-2-furanone	C-1'	HPLC
 33	base propenoate	C-3'	HPLC
 24	oligonucleotide 3'-phosphoglycaldehyde	C-3'	PAGE
 9	oligonucleotide 3'-phosphoglycolate	C-4'	PAGE
 10	base propenal	C-4'	reaction with thiobarbituric acid
 56	Nucleotide 5'-aldehyde	C-5'	PAGE
 59	fufural (FUR)	C-5'	HPLC

Table 1: Unique DNA Scission Products.

Principle of Gel Electrophoresis: DNA is a negatively charged molecule. If put DNA into an electric field, DNA will move from the negative to the positive pole. A gel serves as the matrix for the movement of the DNA molecule. The gel is a semisolid material with certain size pores. Plasmid DNA structure consists of three forms, Form I, supercoiled; Form

II, relaxed and Form III, linear (Figure 1.17). The supercoiled form is able to move faster through the pores of the gel than linear and relaxed form. Because the different mobility, we can identify the plasmid DNA structure in gel. Furthermore, we can use the method to test the ability of compound cleavage DNA.

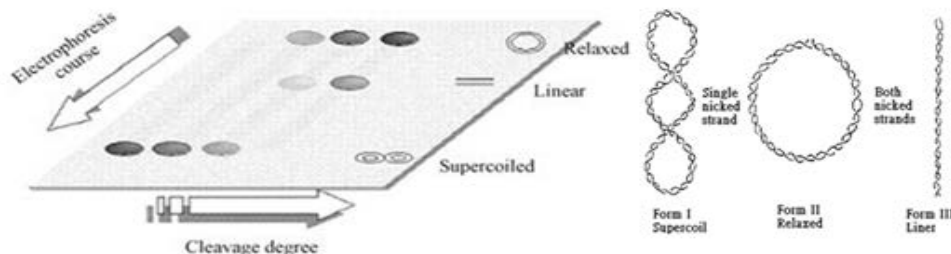


Figure 1.17: Typical electrophoresis gel appearance in the cleavage of plasmid DNA.

Principle of Maxam-Gilbert Sequencing: Around 1977, Wally Gilbert (Harvard) and his technician Allan Maxam developed chemical sequencing. This method requires radioactive labeling at one end and purification of DNA fragment sequenced. Chemical treatment generates breaks at a small proportion of one or two of the four nucleotide bases in each of four reactions (G, A+G, C, C+T) (Table 2). Thus a series of labeled fragments is generated, from the

radiolabeled end to the first 'cut' site in each molecule. The fragments in the four reactions are arranged side by side in gel electrophoresis for size separation. To visualize the fragment, the gel is exposed to X-ray film for autoradiography which yields a series of dark bands and each corresponds to a radiolabeled DNA fragment, from which the sequence may be inferred (Figure 1.18).

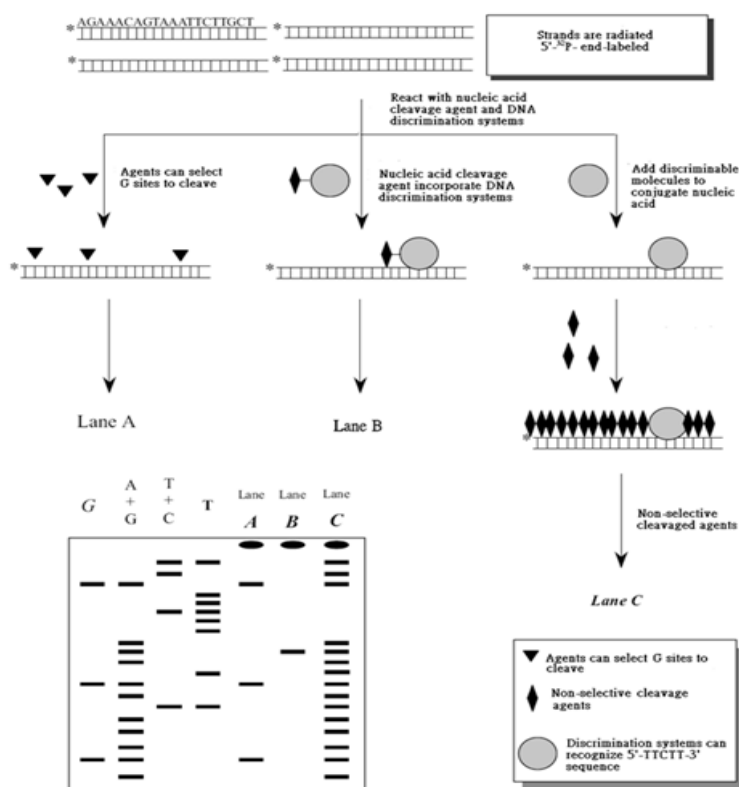


Figure 1.18: Maxam-Gilbert sequencing used for nucleic acid cleavage incorporated DNA discrimination systems (5'-TTCTT-3').

Base specificity	Base reaction	Reaction agent	Chemical used for strand cleavage
G	Alkylation	Dimethyl sulphate	1 M piperidine, 90°C, 30 min
A+G	Depurination	88% Formic acid	1 M piperidine, 90°C, 30 min
C+T	Base ring-open reaction	Hydrazine	1 M piperidine, 90°C, 30 min
C	Base ring-open reaction	Hydrazine, High salt	1 M piperidine, 90°C, 30 min

Table 2: Maxam-Gilbert sequencing.

Motive

Previous report indicates that cantharidin causes oxidative stress to provoke DNA damage in vivo, so we try to use cantharidin and its derivatives to trigger DNA cleavage by irradiation. Some of materials exhibiting planet aromatic compound were also determined to test whether it can cleave DNA strand or not. In the mean-time, we would like to endeavor on the mechanism of the critical molecular pathways of DNA damages. Ultimately, we would like to develop chemical nucleases to apply to anticancer or gene therapy in the future.

Materials and Methods

Extract Cantharidin from Beetles (Table 3)

Materials	Source
Celite 545	Merck
Ethanol	Mallinckrodt
Ethyl acetate	Mallinckrodt
Methanol	Mallinckrodt

Table 3: Cantharidin from Beetles.

Instrument:

- Hot plate : IKA LABORTECHNIK
- Heating Bath B-490
- Rotavapor R-200
- Low Temperature Thermostatic Water baths

The preparation of Cantharidin (Figure 2.1).

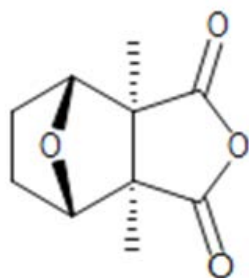


Figure 2.1: Structure of cantharidin.

We added *Mylabris* (0.5Kg) into 50% EtOH and concentrated it by evaporator. After concentrating, we extract H₂O layer from the mixture and filtrated the layer by celite filter. The filtrate will partition into H₂O layer and EtOAc layer by added EtOAc. Finally, we collected the EtOAc layer and concentrated the layer by evaporator. The residues were being recrystallized with MeOH and produced cantharidin (0.5g). Finally, we got white crystal. Yield: 0.1% m.p: 216-218°C (MeOH); ¹H NMR (CDCl₃, 500MHz): δ 1.24 (s, 6H, CH₃×2), δ 1.74-1.81 (m, 4H, CH₂×2), δ 4.73 (t, 2H, J=3.0, 1.8Hz, OCH×2).

Synthesis (Table 4)

Materials	Source
2-4(-Aminophenyl)-6-methyl-benzothiazole	Aldrich
Cantharidin	Dried bodies of beetles
Dichloromethane	Merck
Hexane	Merck
1,8-Naphthalic anhydride	Alfra aesar
p-phenylenediamine	Sigma
Toluene	
Triethylamine	Merck

Table 4: Materials & Source of Cantharidin.

Instrument:

- 2-Decimal Balance: METTLER YOLED0, AG 245
- 4-Decimal Balance: METTLER YOLED0, AG 204
- Hot plate : IKA LABORTECHNIK
- Thick-walled glass
- Teflon tank
- Seal steel-made container
- Microprocessor temperature controller: MAXTHERMO MC-2838

The preparation of 2,6-Dimethyl-4-[4-(6-methyl-benzothiazol-2-yl)-phenyl]-10-oxa-4-aza-tricyclo [5.2.1.0] decane-3,5-dione (compound D) (Figure 2.2).

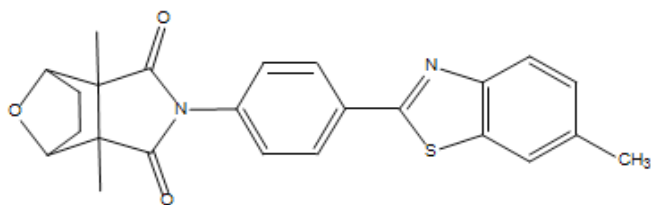


Figure 2.2: Structure of 2,6-Dimethyl-4-[4-(6-methyl-benzothiazol-2-yl)-phenyl]-10-oxa-4-aza-tricyclo [5.2.1.0] decane-3,5-dione (compound D)

We added cantharidin 196 mg (196.2 g/mol) and 2-(4-Aminophenyl)-6-methyl-benzothiazole 264 mg (240.33g/mol) in 2ml triethanolamine and sealed those mixture into a thick-walled glass tube. After heating the tube to 200°C for 2.0 h, open the lid and cool the tube to room temperature. Continue heating to 190°C for 1.0h to evaporate H₂O. Finally, we will get black and sticky mixture (337mg). The mixture was separated by PTLC.

The Layer chromatography was performed under dichloromethane/ ethyl acetate 18:1(by vol.) as its solvent system. Then, the PTLC plate was sunk into solvent to separate products. After heating the plate, the sample was able to identify as dark-yellow band on PTLC plates. Scrape of the products from PTLC and mix with CH₂Cl₂. Finally, we filtered off the silica and dried the CH₂Cl₂ solvent to obtain crystals (yellow solid) Yield: 48%; MS m/z (rel. int.) 418.14[M]⁺ (100) PTLC R_f: 0.85 (Figure 2.3).

The Preparation of N-(4-Amino-Phenyl)-Benzo[De] Isoquinoline-1,3-Dione (Compound K)

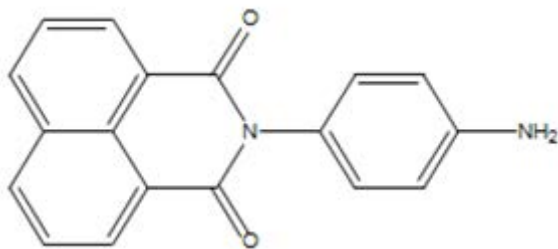


Figure 2.3: Structure of N-(4-Amino-phenyl)-benzo[de] isoquinoline-1,3-dione (compound K).

We add 198 mg 1,8-Naphthalic anhydride (198.17 g/mol) and 119 mg p-phenylenediamine (108.14 g/mol) into 2 ml triethanolamine and 8 ml toluene. Then, we seal those mixture into a Teflon tank and heated it to 180°C for

3hr. Cooled it to room temperature slowly. After cooling, we discarded the solvent and get precipitate. The precipitate was transferred into a clean tank and added CH₂Cl₂ to dissolve it. The dissolved mixture was separated by PTLC. The products (148 g) were obtained in 75% yield.

The Layer chromatography was performed under dichloromethane/ hexane 1:1 (by vol.) as its solvent system. Then, the PTLC plate was sunk into solvent to separate produce. After heating the plate, the sample was able to identify as brown band on PTLC plates. Scrape of the products from PTLC and mix with CH₂Cl₂. Finally, we filtered off the silica and dried the CH₂Cl₂ solvent to obtain crystals.

White crystal. Yield: 75% m.p: 295-297°C (MeOH); ¹H NMR (CDCl₃, 500MHz): δ 6.80(2H,d, J=8.8Hz,phenyl H3',H5'), 7.06(2H,d, J=8.6Hz,phenyl H-2',H-6'), 7.77(2H,t, J=7.7Hz,H-5,H-8),8.23(2H,d, J=8.0Hz,H-6,H-7), 8.62(2H,t, J=6.7Hz,H-4,H-9).

The Growth of *Escherichia coli* (pUC19 DH5α) (Table 5)

Materials	Source
Ampicillin	Amresco
LB broth powder (Miller, Luria Bertani)	Bio Basic

Table 5: Materials & Source of *E. coli*.

Instrument:

- 2-Decimal Balance: METTLER YOLED0, AG 245
- 4-Decimal Balance: METTLER YOLED0, AG 204
- Water Purification systems: BIBBY-A400 (RO) & Millipore Milli-Q Plus (DI)
- Oven: DENG YNG, Drying Oven DOS60
- Autoclave: TOMIN, TM-329,121°C, 1.2 Kg/cm²
- Orbital Shaker Incubator: FIRSTEK SCIENTIFIC, S300R
- BSC: 4BH-24

The pUC19 plasmid was transformed to *E.coli*. We added 5μl pUC19 plasmid to a 50μl solution of DH5α competent cell, put in an ice bath for 5 min, and in a 42°C bath for 2 min with heat stock. Finally 100μl LB was added, and the mixture was incubated at 37°C, 10 min. We collected 50μl broth and spread it on a LB(Amp) plate by glass beads at 37°C incubate it overnight. After incubating the plate, we selected one survival colony to transfer it to 3ml LB and incubate it for 16~18 hr. We added the 3 ml LB mixture to 100 ml LB and incubate it in 37°C, 220 rpm condition till OD= 0.8.

Purification Plasmid DNA (Table 6)

Materials	Source
Midiperp Kit solution I	GeneMark
Midiperp Kit solution II	GeneMark
Midiperp Kit solution III	GeneMark
Chloroform	Amresco
Ethanol	Merck
Isopropanol	Mallinckrodt
Phenol	Amresco

Table 6: Plasmid DNA Purification.

Instrument:

- Water Purification systems: BIBBY-A400 (RO) & Millipore Milli-Q Plus (DI)
- Oven: DENG YNG, Drying Oven DOS60
- Autoclave: TOMIN, TM-329, 121°C, 1.2 Kg/cm²
- Vortex: FINEVORTEX
- Low Temperature Freezer: 4°C, FIRSTEK SCIENTIFIC, CC-2; -20°C: White-Westinghouse
- Spin
- Centrifuge: Labnet MODLE:24D; Beckman, Coulter Optima L-90K Ultracentrifuge
- Rotor: SLA 1500
- Ultraviolet-Visible Spectrophotometer: HP 8453

The harvested cells were separated by centrifuge (8000rpm, 10min). Pellet, which contained cells, we used 10ml Midiperp Kit solution I to resuspend and react it for 10 min in room temperature. The 10ml Midiperp Kit solution II was added to mixture and reacted it for 10 min. After reaction, 10ml Midiperp Kit solution III was added to mixture and denatured proteins, cell remains, and chromosome DNA etc. By centrifuging (8000 rpm, 10min), we can obtain supernatant liquor, which contained pUC19 plasmid DNA. In order to precipitate the rough pUC19 plasmid DNA, we added 24 ml isopropanol and centrifuged (12000 rpm, 10 min). We used 100µl D.I. Water to dissolve the rough pUC19 plasmid (white pellet) and added 100µl phenol & chloroform mixture. After centrifuging, we got supernatant

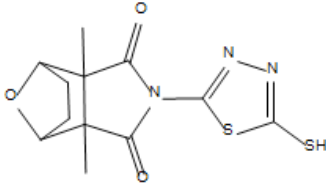
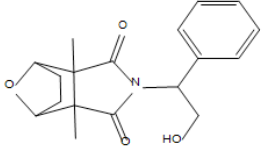
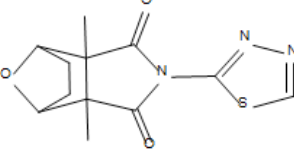
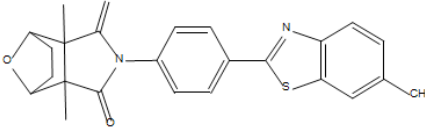
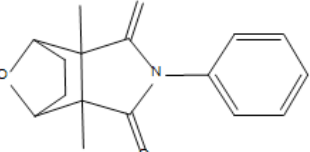
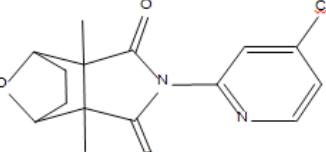
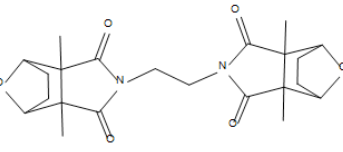
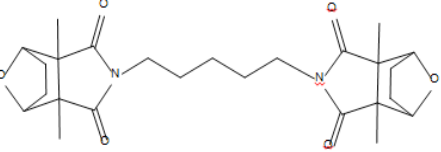
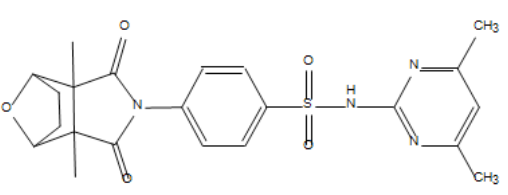
liquor and added 100µl chloroform to precipitate impurities. We selected supernatant liquor and used 80µl isopropanol to precipitate pure pUC19 plasmid. Finally, we collected the pellet by centrifuging and used D.I. Water to dissolve it. We also processed dialysis to obtain more pure pUC19 plasmid DNA and used UV-vis spectrometry (Ratio=260/280) to identify the degree of purity (Figure 2.4).

Photoreaction & DNA Cleavage Studies via Supercoiled Plasmid (Table 7 & 8)

Materials	Source
Agarose I	Amresco
Boric Acid	RDH
Cantharidin	Lin P. Y.'s lab
Compound A	Lin P. Y.'s lab
Compound B	Lin P. Y.'s lab
Compound C	Synthesized
Compound D	Lin P. Y.'s lab
Compound E	Lin P. Y.'s lab
Compound F	Lin P. Y.'s lab
Compound G	Lin P. Y.'s lab
Compound H	Lin P. Y.'s lab
Compound I	Lin P. Y.'s lab
Compound J	Lin P. Y.'s lab
Compound Q (N-(4-Amino-phenyl)-benzo[de]isoquinoline-1,3-dione)	Synthesized
Compound T (3-Amino-5-phenylpyrazole)	Acros
Dimethyl sulfoxide (DMSO)	Amresco
Ethidium bromide	Amresco
[Ethylenedinitrilo]-tetraacetic acid disodium salt	Mallinckrodt
Hydrochloric acid	RDH
Tris	Amresco
1 kb DNA Ladder	Protech

Table 7: DNA Cleavage Studies.

Compounds	Structures
Cantharidin	

Compound A	
Compound B	
Compound C	
Compound D	
Compound E	
Compound F	
Compound G	
Compound H	
Compound I	

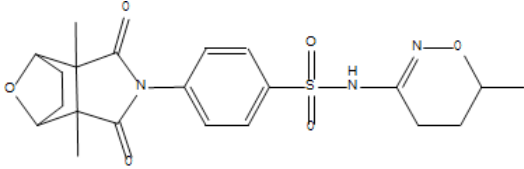
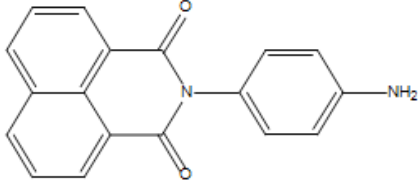
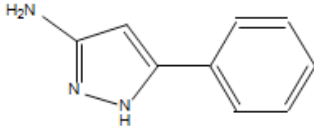
Compound J	
Compound K (N-(4-Amino-phenyl)-benzo[de]isoquinoline-1,3-dione)	
Compound L (3-Amino-5-phenylpyrazole)	

Table 8: Structures of Cantharidin and Compound A~V.**Instrument:**

- 4-Decimal Balance: METTLER YOLEDO, AG 204
- Water Purification systems: BIBBY-A400 (RO) & Millipore Milli-Q Plus (DI)
- Oven: DENG YNG, Drying Oven DOS60
- Agar Horizontal gel Electrophoresis
- Electrophoresis Power Source: GE 100
- Photo-documentation system: Electronic case; MITUBISHI, P91W; DOC-print CCD F590 180x240
- Photochemical Reactor PR 2000
- pH Meter: SUNTEX pH/ORP Meter
- Microwave oven: SAMPO

Supercoiled pUC19 plasmid (1mg/mL) was reacted with varieties of concentration of those compounds (1 μ M~1000 μ M) by irradiating UV light (352nm) at room temperature for 1hr. After photoreaction, we analyzed the cleaving abilities of those compounds by gel electrophoresis. To the reaction mixture was added gel-loading buffer (2 μ L containing 0.25% bromophenol blue, 0.25% xylene cyanol, and 30% glycerol). Then the reaction mixture was loaded on 1% agarose gel with ethidium bromide staining. The electrophoresis tank was attached to a power supply at current (100mA). The gel was visualized by 312-nm UV transilluminator and photographed by photo documentation system. Quantitation of DNA cleavage was performed by integration of the optical density as function of the band area by use of Scion Image program.

Explore the DNA Cleavage with Site Specificity (Table 9)

Materials	Source
40% Acrylamide/Bis solution, 29:1	BIO-RAD
Ammonium per sulfate (APS)	Amresco
Acetic acid	Merck
Boric acid	RDH
Bromphenol blue	Sigma
5'end labeled biotin-DNA	Protech
5'end labeled 6-FAM-DNA	Protech
Dimethyl sulfate (DMS)	Merck
Ethanol	Merck

[Ethylenedinitrilo]-tetracetic acid disodium salt	Mallinckrodt
Formic acid 88%	J.T.Baker
Formamide	J.T.Baker
Hydrazine	Acros
HIV-27 DNA (5' labeled biotin)	Protech technology
Isopropanol	Mallinckrodt
Methanol	Merck
β -mercaptoethanol	Sigma
Pipridine	Merck
Sodium cacodylate trihydroate	Sigma
Sodium acetate anhydrate	Fluka
Sodium dodecyl sulfate (SDS)	Amresco
Sodium chloride	RDH
tRNA	Sigma
TEMED	Plus one
Tris	Amresco
Urea	Sigma
Xylene cyanol FF.	Sigma
Nylon transfer membrane	Millipore
Filter paper	Toyo Roshi Kaisha, Ltd.
Panomics' EMSA Kit	Panomics'

Table 9: DNA Cleavage with Site Specificity.

Instrument:

- 4-Decimal Balance: METTLER YOLEDO, AG 204
- Water Purification systems: BIBBY-A400 (RO) & Millipore Milli-Q Plus (DI)
- Oven: DENG YNG, Drying Oven DOS60
- Spin
- SDS Vertical Slab Gel Electrophoresis
- Electrophoresis Power Source: Bio-Rad
- Orbital Shaker: FIRSTEK S-101
- pH Meter: SUNTEX pH/ORP Meter
- PCR machine: Biometra T3 Thermo cyclor
- pH Meter: SUNTEX pH/ORP Meter
- Low Temperature Freezer: 4°C, FIRSTEKSCIENTIFIC, CC-2; -20°C: White-Westinghouse
- ECL Semi-dry Blotters: Amersham Biosciences
- CL-1000 Ultraviolet Crosslinker: UVP
- Typhoon: 9410

To explore the DNA cleavage with site specificity, we use the HIV-27 DNA, which labeled the 5'-terminus of oligonucleotide (5'-GCAGATCTGAGCCTGGGAGCTCTCTGC-3') with biotin [36]. The reaction mixture containing 5'-end labeled biotin-DNA solution (50 μ M), a phosphate buffer

(0.10 M, pH 5.0) and compound D (1mM) in Pyrex vial were irradiated with 352-nm UV at room temperature for 1.0hr, the reaction mixtures were quenched with 95% EtOH. The solutions were then subjected to piperidine treatment and ethanol precipitation. The DNA pellet was re-suspended in aqueous piperidine solution (10% 70 μ L) and maintained at 95°C for 30 min. Subsequently, the reaction mixtures were sequentially lyophilized, treated with water (30 μ L), lyophilized, and re-suspended in the formamide loading buffer (80% formamide, 0.25% bromophenol blue, and 0.25% xylene cyanol). The DNA solution and Maxam-Gilbert markers were analyzed by use of 20% polyacrylamide/7M urea gel. The electrophoresis was performed at voltage of 250 V for 1 hr. The 20% polyacrylamide/8M urea gel was transferred to nylon membrane by ECL semi-dry blotters. The DNA solution and Maxam-Gilbert markers produced chemiluminescence by Panomics' EMSA kit protocol. The cleavage positions were visualized by use of Kodak X-Omat Ar-5 film.

We also use the HIV-27 DNA labeled 5'-terminus of oligonucleotide with 6-FAM (6-Carboxyfluorescein) to proceed experiment. The reaction mixture containing 5'-end

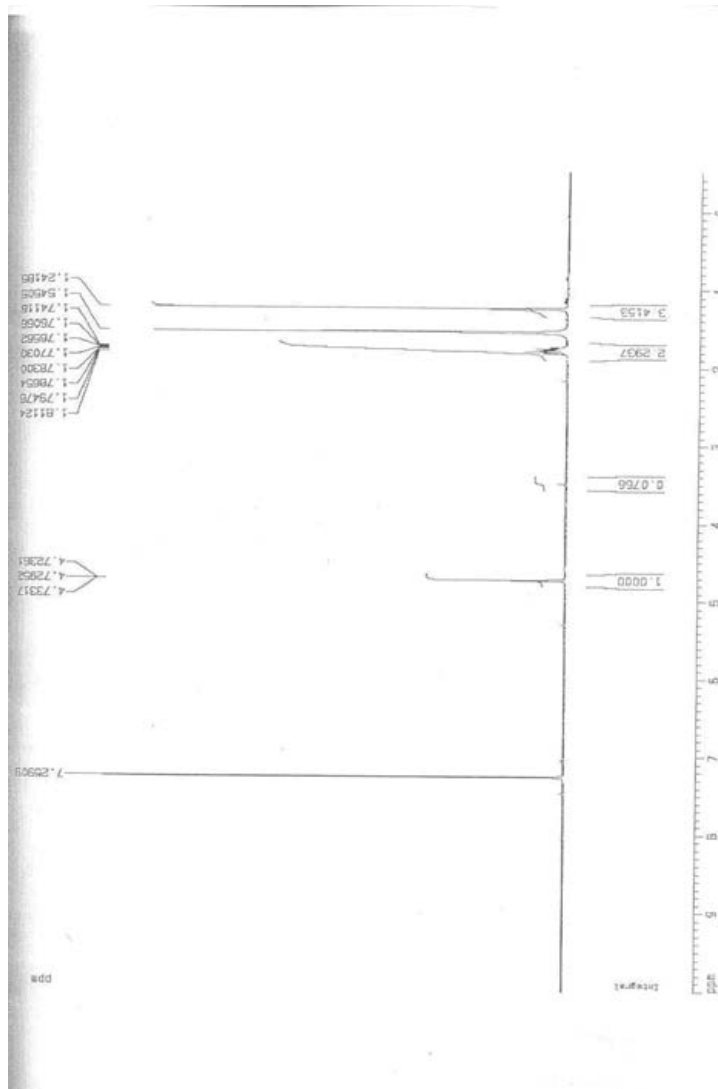
labeled 6-FAM-DNA solution (20 μ M), a phosphate buffer (0.10 M, pH 5.0) and compound D (100 μ M) in Pyrex vial were irradiated with 352-nm UV at room temperature for 1.0hr, the reaction mixtures were quenched with 95% EtOH. The solutions were then subjected to piperidine treatment and ethanol precipitation. The DNA pellet was resuspended in aqueous piperidine solution (10% 70 μ L) and maintained at 95°C for 30 min. Subsequently, the reaction mixtures were sequentially lyophilized, treated with water (30 μ L), lyophilized, and resuspended in the formamide loading buffer (80% formamide, 0.25% bromophenol blue, and 0.25% xylene cyanol). The DNA solution and Maxam-Gilbert markers were analyzed by use of 20% polyacrylamide/7M urea gel. The electrophoresis was performed at voltage of 250 V for 1 hr. After electrophoresis, we use 488-nm light to excite 6-FAM and detected the emission wave light (518-nm)

by typhoon.

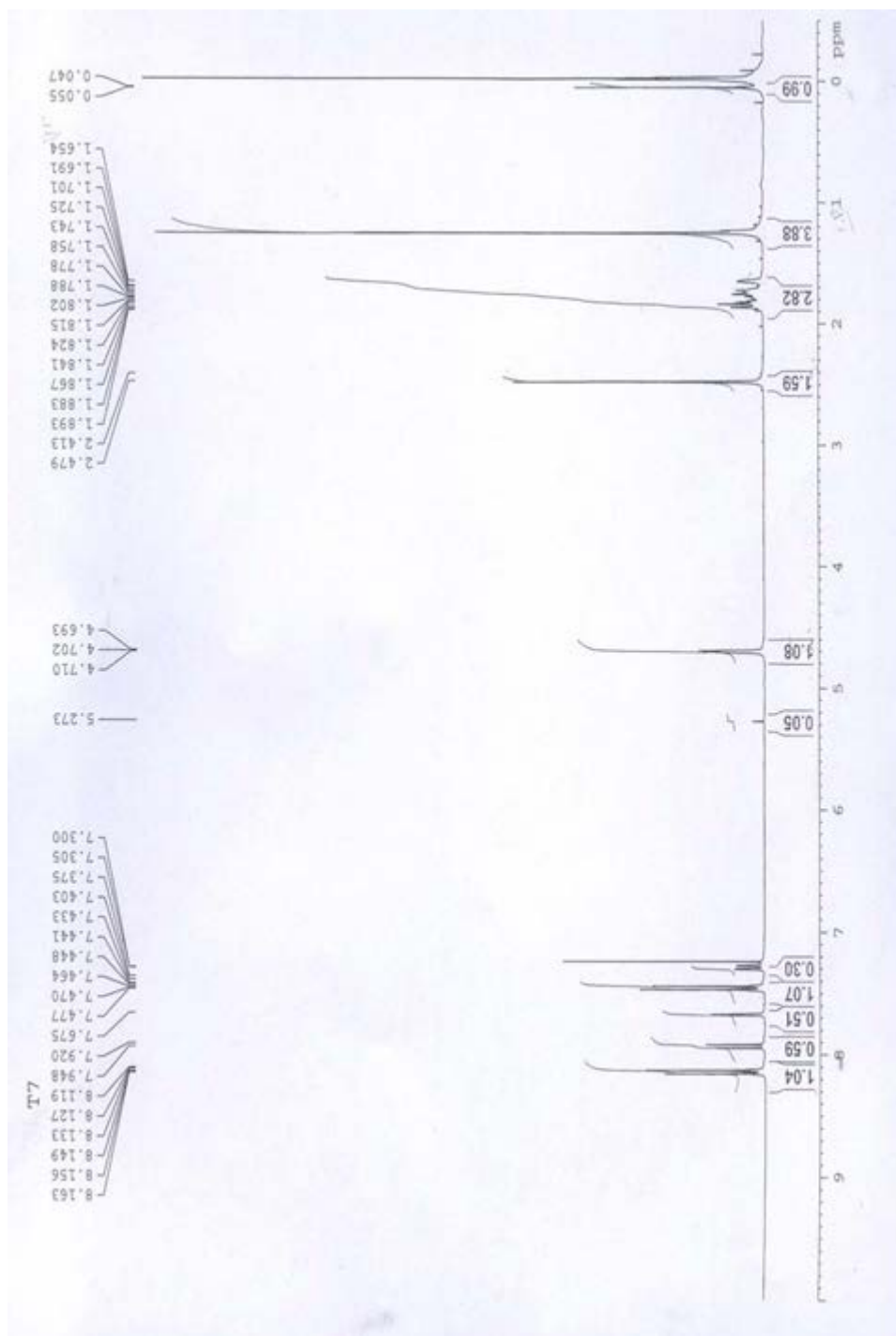
Results and Discussion

Synthesis

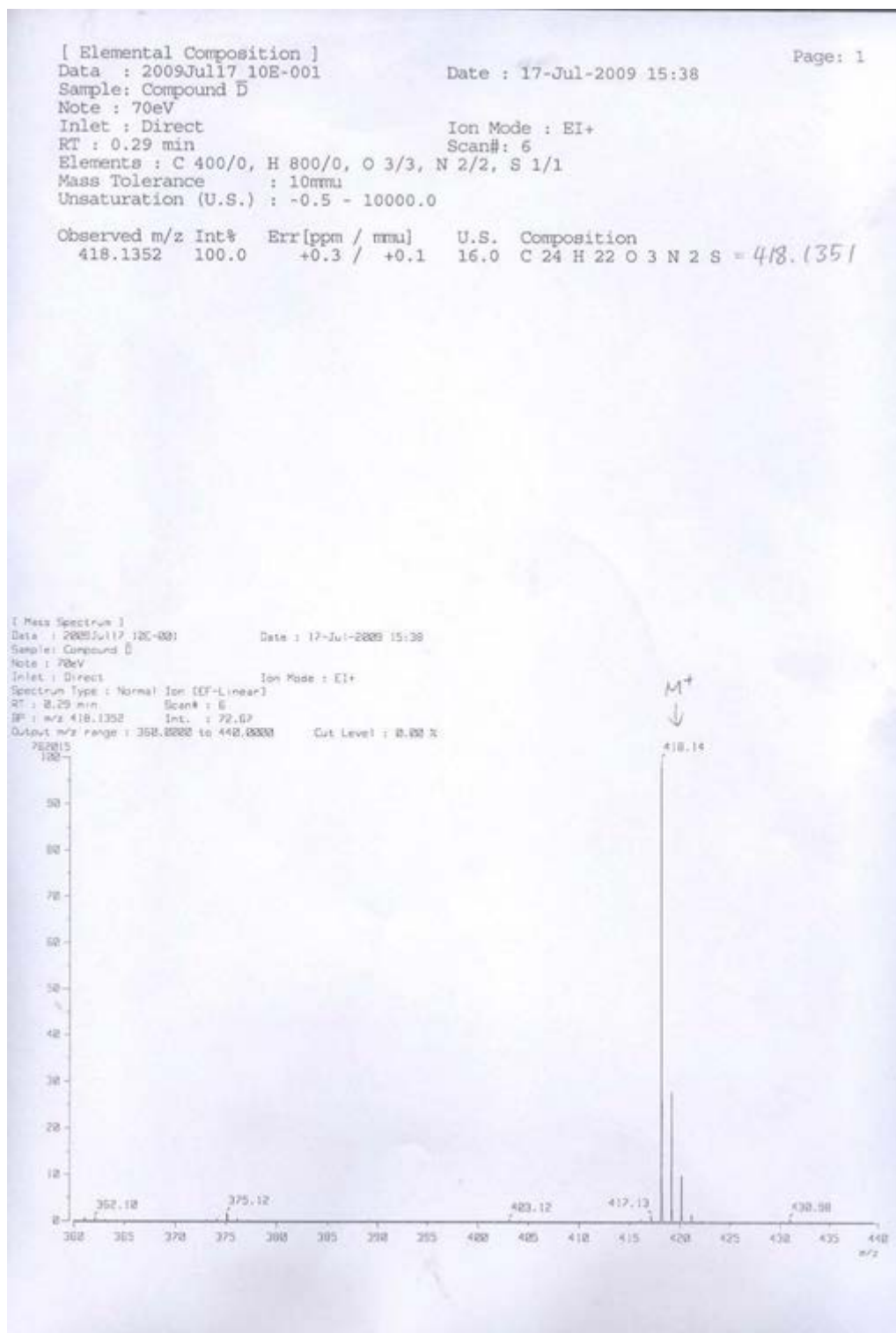
The cantharidin was isolated from dried bodies and prepared cantharidin derivatives using the pressure technique synthesis. We utilized the hydrothermal method to synthesize 8-Naphthalic anhydride derivatives. The method of extract cantharidin from *Mylabris phalerata Pall* is safer than High-Pressure Diels-Alder Reaction, Here, we could obtain 0.5g cantharidin and identified by NMR (Appendix 1). In addition, we use a simple procedure for preparation of cantharidin derivatives 1,8-Naphthalic anhydride derivatives and identify those compound by H-NMR (Appendix 2-5).



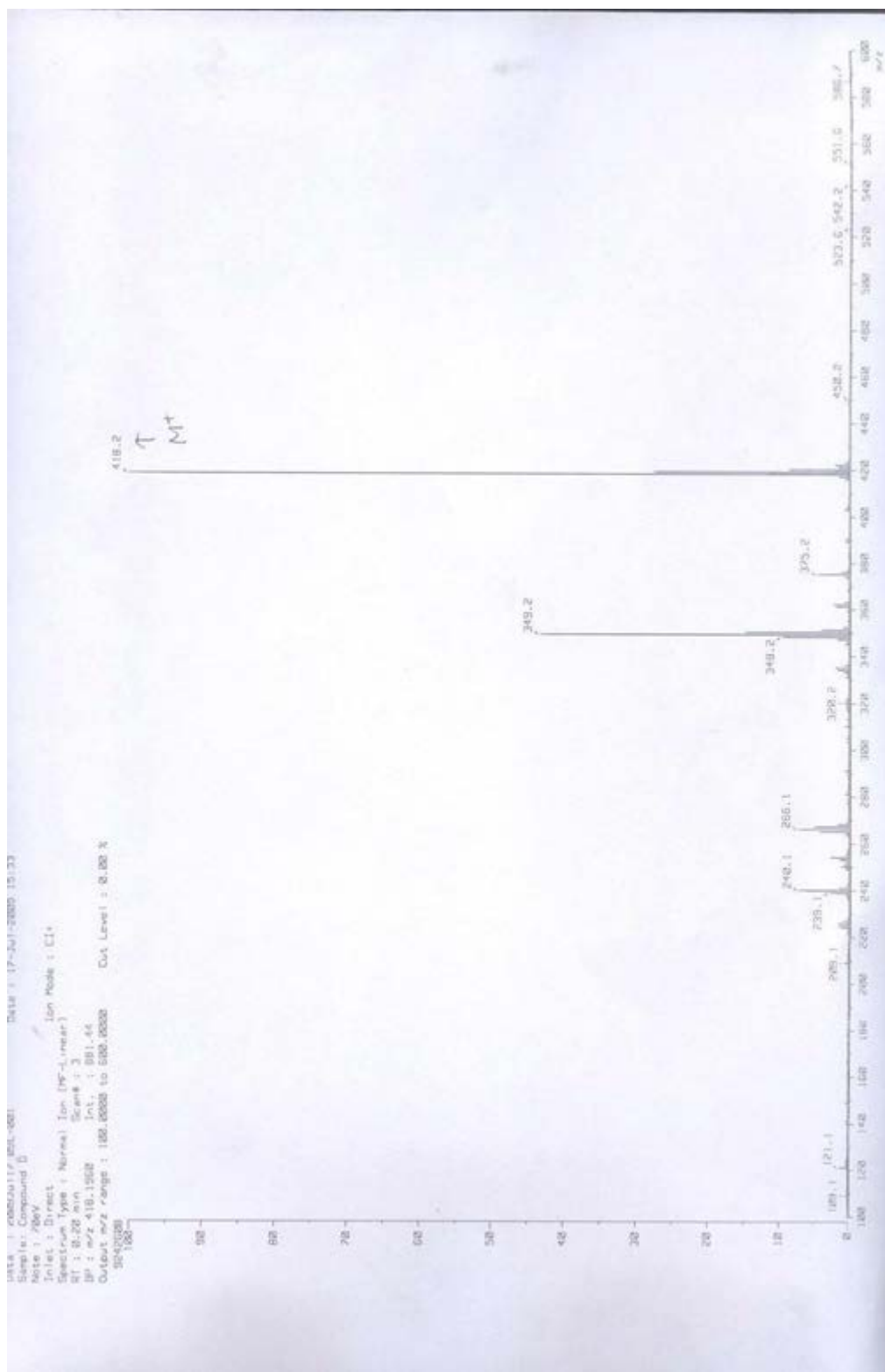
Appendix 1: ¹H-NMR spectrum of cantharidin (CDCl₃, 500 MHz).



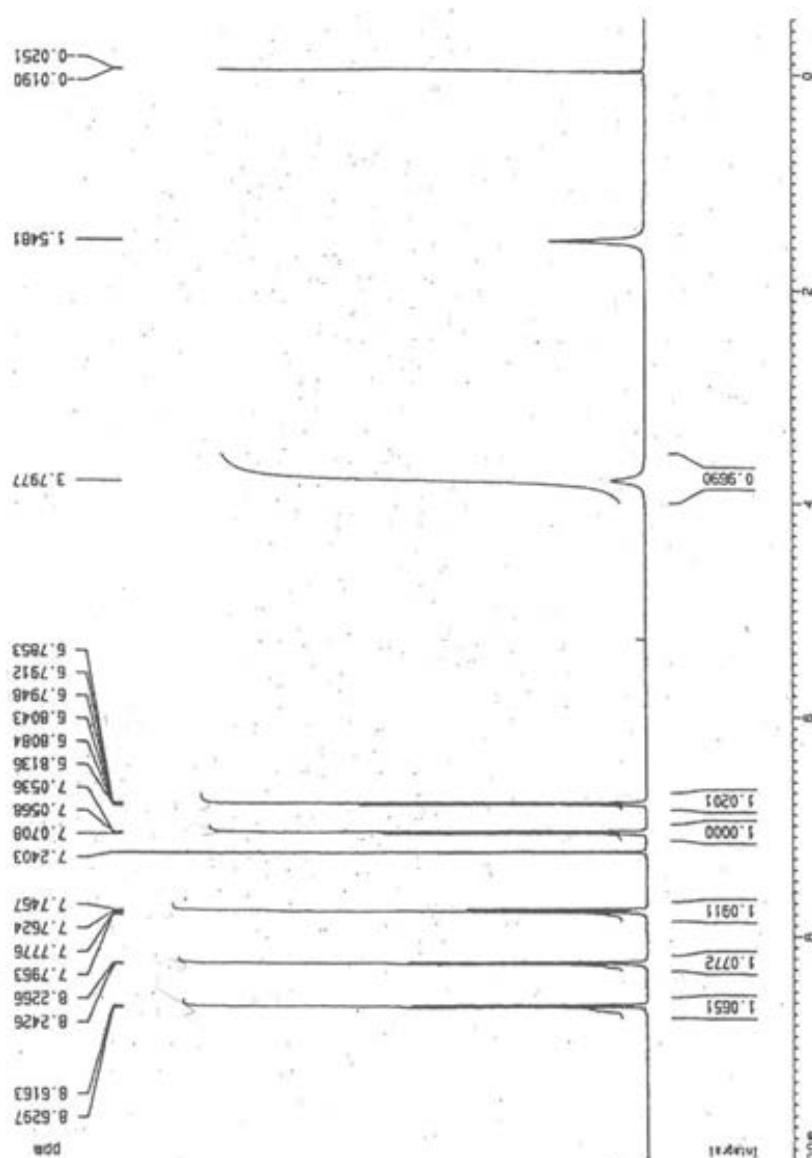
Appendix 2: ¹H-NMR spectrum of compound D (CDCl₃, 300 MHz).



Appendix 3: LRMS spectrum of Compound D (EI).



Appendix 4: LRMS spectrum of Compound D (FAB).



Appendix 5: $^1\text{H-NMR}$ spectrum of compound K (CDCl_3 , 400 MHz).

Prepare Super-Coiled DNA

The *E. coli* (DH5 α) containing pUC19 plasmid was cultured in LB medium with ampicillin for 12~16h. After incubating and centrifuging, we got about 0.29 mg/ml bacteria pellet (wet weight). Then, we used different solvents to extract the plasmid. Notably, the extracted plasmid was affected with irradiating with UV light (352-nm) (Figure 3.1).

We surmised that the plasmid contained some impurities which may cause radiation- sensitivity. To remove the impurities, the extracted plasmid was dialysed. Compare with the commercial plasmid, we could use the easier and cheaper method to get a great quantity of plasmid with high purity.

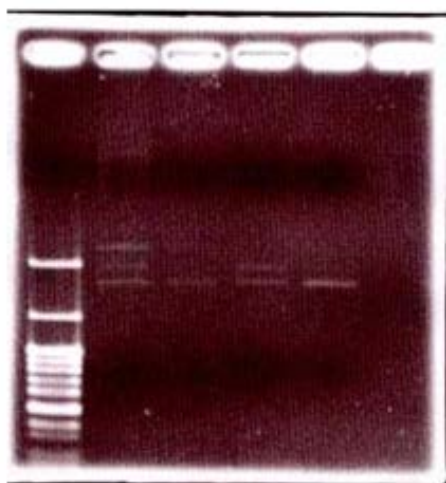


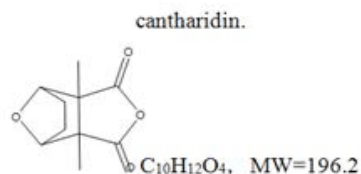
Figure 3.1: The differences of pUC 19 plasmid DNA proceed dialysis before and after. Land 1. Marker Land 2. pUC19 plasmid DNA, before dialysis, UV= 352-nm, 1hr. Land 3. pUC19 plasmid DNA, after dialysis, UV= 352-nm, 1hr. Land 4. pUC19 plasmid DNA, before dialysis, UV= 352-nm, 1hr. Land 5. pUC19 plasmid DNA, after dialysis, UV= 352-nm, 1hr.

DNA Cleavage Studies Mediated by Cantharidin Derivatives Using Supercoiled Plasmid pUC19

According to the previous literature, Cantharidin was found that it could cleavage DNA in cell. But the detail mechanism is still not clear. Here, we use cantharidin and its derivatives (compound A~L) to explore the mechanism and also want to know all of them could be serves as photo-induced DNA cleavage agents. The pUC19 plasmid was used as DNA source for investigating the behavior of these compounds. All of these compounds were dissolved in DMSO as stoke solution. Then, the stoke solutions were added to the supercoiled plasmid (Form I) solution to the final concentration of 1mM and irradiated with or without irradiation ($\lambda=352\text{-nm}$) at room temperature for 1hr.

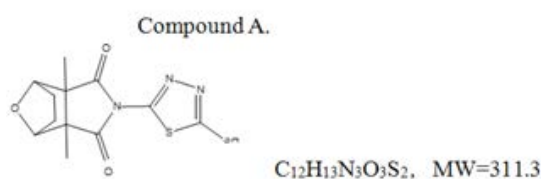
After reaction, the results were analyzed by gel electrophoresis. The results from gel electrophoresis showed that cantharidin and compound A, B, C, E, F, G, H, K and L could not cleavage pUC19 plasmid by single-strand scission with irradiation (Appendix 6-17). These indicated that they may adopt other mechanism to cleavage DNA. Compound D, I, and J could cleavage the plasmid through single-strand scission and produce the relaxed circular DNA (from II). Compare the efficiency, compound D exhibited the highest cleaving efficiency (Figure 3.2-3.5) and compound I and compound J (Appendix 14 and 15) only exhibited a little cleaving efficiency under acidic condition (pH=5.0 and pH=6.0).

Land 1: Marker. Land 2: Control. Land 3: 10mM phosphate buffer, pH=5.0, dark, 1hr. Land 4: 10mM phosphate buffer, pH=5.0, UV=352 nm, 1hr. Land 5: 10mM phosphate buffer, pH=6.0, dark, 1hr. Land 6L 10mM phosphate buffer, pH=6.0, UV=352nm, 1hr. Land 7: 10mM phosphate buffer, pH=7.0, dark 1hr. Land 8: 10mM phosphate buffer, pH=7.0, UV=352 nm, 1hr. Land 9: 10mM phosphate buffer, pH=8.0, dark, 1hr. Land 10: 10mM phosphate buffer, pH=8.0, UV=352 nm, 1hr. Land 11: 10mM phosphate buffer, pH=9.2, dark, 1hr. Land 12: 10mM phosphate buffer, pH=9.2, UV=352 nm, 1hr.



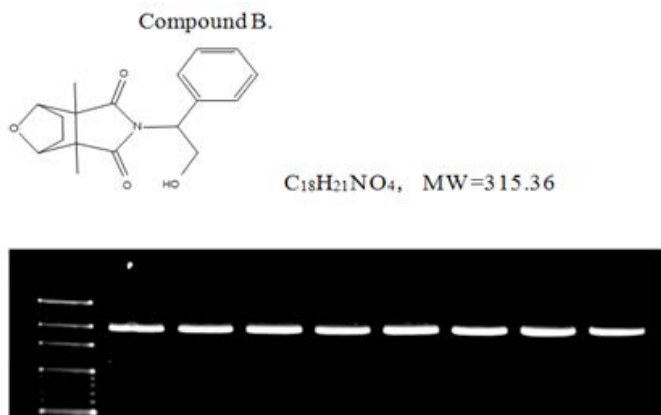
Appendix 6: Gel retardation assay of plasmid pUC19 in presence of 1mM.

Land 1: Marker. Land 2: Control. Land 3: 10mM phosphate buffer, pH=6.0, dark, 1hr. Land 4: 10mM phosphate buffer, pH=6.0, UV=352 nm, 1hr. Land 5: 10mM phosphate buffer, pH=7.0, dark, 1hr. Land 6: 10mM phosphate buffer, pH=7.0, UV=352 nm, 1hr. Land 7: 10mM phosphate buffer, pH=8.0, dark, 1hr. Land 8: 10mM phosphate buffer, pH=8.0, UV=352 nm, 1hr.



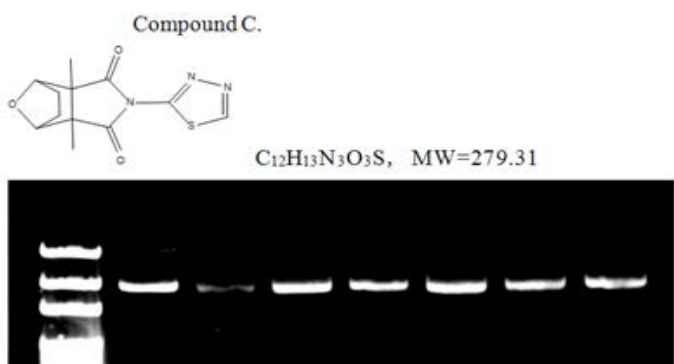
Appendix 7: Gel retardation assay of plasmid pUC19 in presence of 1mM.

Land 1: Marker. Land 2: Control. Land 3: 10mM phosphate buffer, pH=6.0, dark, 1hr. Land 4: 10mM phosphate buffer, pH=6.0, UV=352 nm, 1hr. Land 5: 10mM phosphate buffer, pH=7.0, dark, 1hr. Land 6: 10mM phosphate buffer, pH=7.0, UV=352nm, 1hr. Land 7: 10mM phosphate buffer, pH=8.0, dark, 1hr. Land 8: 10mM phosphate buffer, pH=8.0, UV=352 nm, 1hr.



Appendix 8: Gel retardation assay of plasmid pUC19 in presence of 1mM.

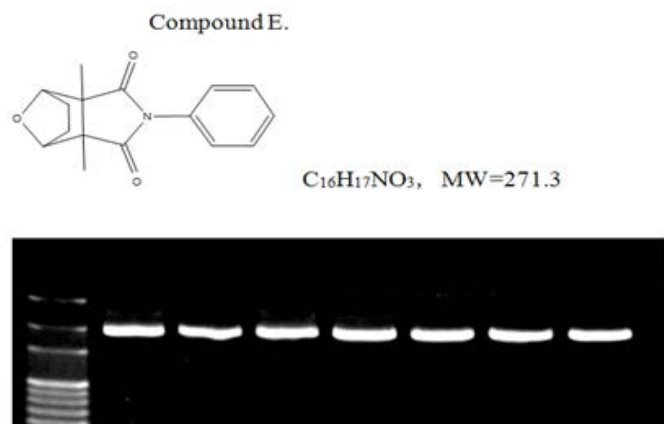
Land 1: Marker. Land 2: Control. Land 3: 10mM phosphate buffer, pH=6.0, dark, 1hr. Land 4: 10mM phosphate buffer, pH=6.0, UV=352 nm, 1hr. Land 5: 10mM phosphate buffer, pH=7.0, dark, 1hr. Land 6: 10mM phosphate buffer, pH=7.0, UV=352 nm, 1hr. Land 7: 10mM phosphate buffer, pH=8.0, dark, 1hr. Land 8: 10mM phosphate buffer, pH=8.0, UV=352 nm, 1hr.



Appendix 9: Gel retardation assay of plasmid pUC19 in presence of 1mM.

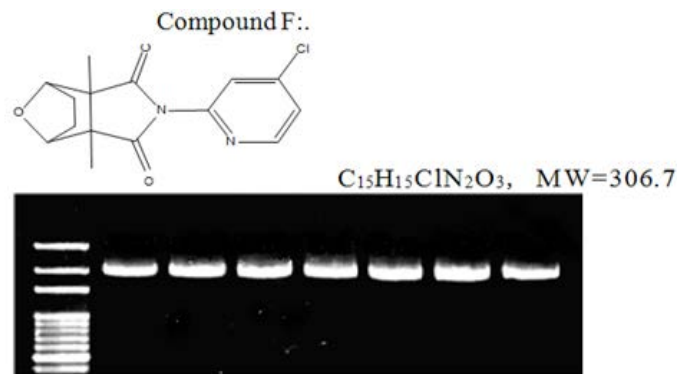
Land 1: Marker. Land 2: Control. Land 3: 10mM phosphate buffer, pH=6.0, dark, 1hr. Land 4: 10mM phosphate buffer, pH=6.0, UV=352 nm, 1hr. Land 5: 10mM phosphate buffer, pH=7.0, dark, 1hr. Land 6: 10mM phosphate buffer, pH=7.0, UV=352 nm, 1hr. Land 7: 10mM phosphate buffer, pH=8.0, dark, 1hr. Land 8: 10mM phosphate buffer, pH=8.0, UV=352 nm, 1hr.

UV=352 nm, 1hr. Land 7: 10mM phosphate buffer, pH=8.0, dark, 1hr. Land 8: 10mM phosphate buffer, pH=8.0, UV=352 nm, 1hr.



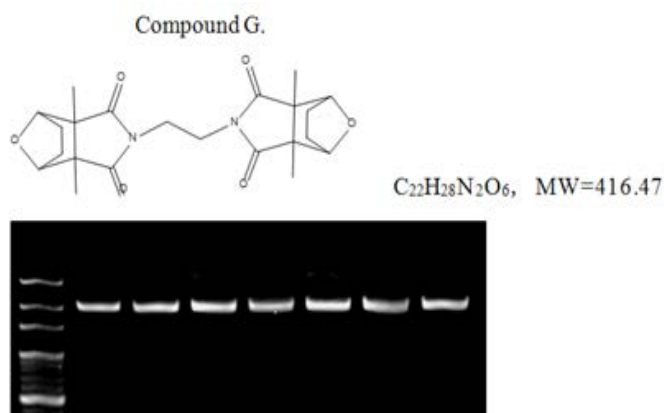
Appendix 10: Gel retardation assay of plasmid pUC19 in presence of 1mM.

Land 1: Marker. Land 2: Control. Land 3: 10mM phosphate buffer, pH=6.0, dark, 1hr. Land 4: 10mM phosphate buffer, pH=6.0, UV=352 nm, 1hr. Land 5: 10mM phosphate buffer, pH=7.0, dark, 1hr. Land 6: 10mM phosphate buffer, pH=7.0, UV=352 nm, 1hr. Land 7: 10mM phosphate buffer, pH=8.0, dark, 1hr. Land 8: 10mM phosphate buffer, pH=8.0, UV=352 nm, 1hr.



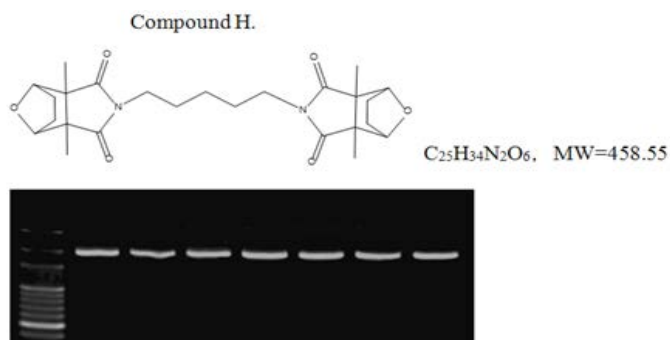
Appendix 11: Gel retardation assay of plasmid pUC19 in presence of 1mM.

Land 1: Marker. Land 2: Control. Land 3: 10mM phosphate buffer, pH=6.0, dark, 1hr. Land 4: 10mM phosphate buffer, pH=6.0, UV=352 nm, 1hr. Land 5: 10mM phosphate buffer, pH=7.0, dark, 1hr. Land 6: 10mM phosphate buffer, pH=7.0, UV=352 nm, 1hr. Land 7: 10mM phosphate buffer, pH=8.0, dark, 1hr. Land 8: 10mM phosphate buffer, pH=8.0, UV=352 nm, 1hr.



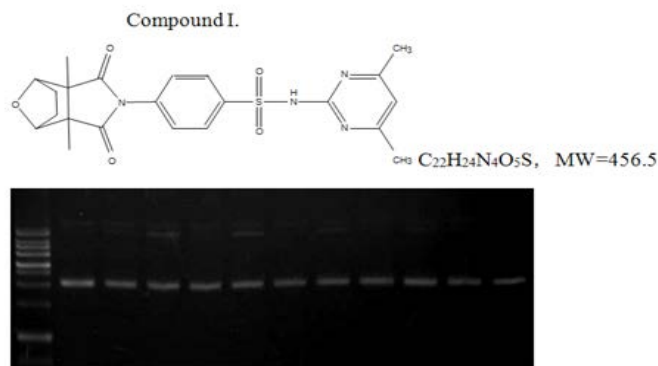
Appendix 12: Gel retardation assay of plasmid pUC19 in presence of 1mM.

Land 1: Marker. Land 2: Control. Land 3: 10mM phosphate buffer, pH=6.0, dark, 1hr. Land 4: 10mM phosphate buffer, pH=6.0, UV=352 nm, 1hr. Land 5: 10mM phosphate buffer, pH=7.0, dark, 1hr. Land 6: 10mM phosphate buffer, pH=7.0, UV=352 nm, 1hr. Land 7: 10mM phosphate buffer, pH=8.0, dark, 1hr. Land 8: 10mM phosphate buffer, pH=8.0, UV=352 nm, 1hr.



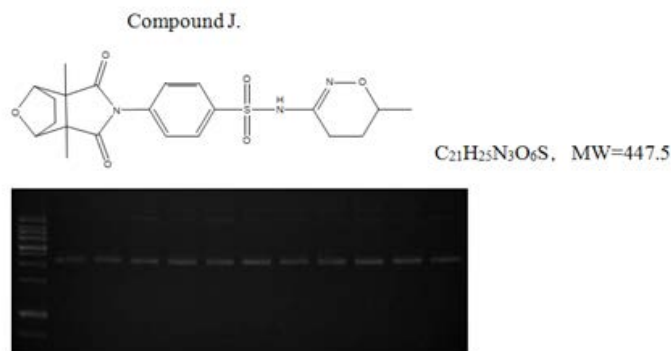
Appendix 13: Gel retardation assay of plasmid pUC19 in presence of 1mM.

Land 1: Marker. Land 2: Control. Land 3: 10mM phosphate buffer, pH=5.0, dark, 1hr. Land 4: 10mM phosphate buffer, pH=5.0, UV=352 nm, 1hr. Land 5: 10mM phosphate buffer, pH=6.0, dark, 1hr. Land 6: 10mM phosphate buffer, pH=6.0, UV=352nm, 1hr. Land 7: 10mM phosphate buffer, pH=7.0, dark, 1hr. Land 8: 10mM phosphate buffer, pH=7.0, UV=352 nm, 1hr. Land 9: 10mM phosphate buffer, pH=8.0, dark, 1hr. Land 10: 10mM phosphate buffer, pH=8.0, UV=352 nm, 1hr. Land 11: 10mM phosphate buffer, pH=9.2, dark, 1hr. Land 12: 0mM phosphate buffer, pH=9.2, UV=352 nm, 1hr.



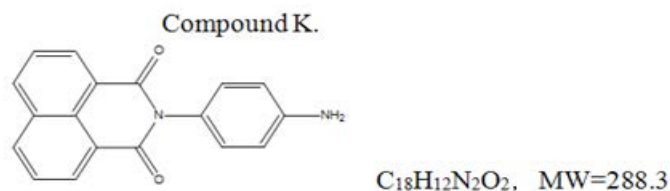
Appendix 14: Gel retardation assay of plasmid pUC19 in presence of 1mM.

Land 1: Marker. Land 2: Control. Land 3: 10mM phosphate buffer, pH=5.0, dark, 1hr. Land 4: 10mM phosphate buffer, pH=5.0, UV=352 nm, 1hr. Land 5: 10mM phosphate buffer, pH=6.0, dark, 1hr. Land 6: 10mM phosphate buffer, pH=6.0, UV=352nm, 1hr. Land 7: 10mM phosphate buffer, pH=7.0, dark, 1hr. Land 8: 10mM phosphate buffer, pH=7.0, UV=352 nm, 1hr. Land 9: 10mM phosphate buffer, pH=8.0, dark, 1hr. Land 10: 10mM phosphate buffer, pH=8.0, UV=352 nm, 1hr. Land 11: 10mM phosphate buffer, pH=9.2, dark, 1hr. Land 12: 0mM phosphate buffer, pH=9.2, UV=352 nm, 1hr.

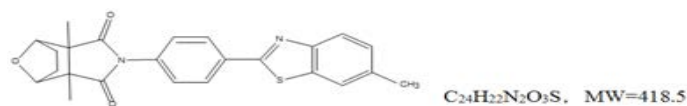


Appendix 15: Gel retardation assay of plasmid pUC19 in presence of 1mM.

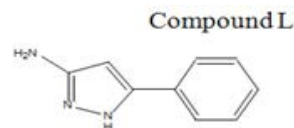
Land 1: Marker. Land 2: Control. Land 3: 10mM phosphate buffer, pH=6.0, dark, 1hr. Land 4: 10mM phosphate buffer, pH=6.0, UV=352 nm, 1hr. Land 5: 10mM phosphate buffer, pH=7.0, dark, 1hr. Land 6: 10mM phosphate buffer, pH=7.0, UV=352 nm, 1hr. Land 7: 10mM phosphate buffer, pH=8.0, dark, 1hr. Land 8: 10mM phosphate buffer, pH=8.0, UV=352 nm, 1hr.



nm, 1hr.



Compound D



Appendix 17: Gel retardation assay of plasmid pUC19 in presence of 1mM.

Appendix 16: Gel retardation assay of plasmid pUC19 in presence of 1mM.

Land 1: Marker. Land 2: Control. Land 3: 10mM phosphate buffer, pH=6.0, dark, 1hr. Land 4: 10mM phosphate buffer, pH=6.0, UV=352 nm, 1hr. Land 5: 10mM phosphate buffer, pH=7.0, dark, 1hr. Land 6: 10mM phosphate buffer, pH=7.0, UV=352 nm, 1hr. Land 7: 10mM phosphate buffer, pH=8.0, dark, 1hr. Land 8: 10mM phosphate buffer, pH=8.0, UV=352

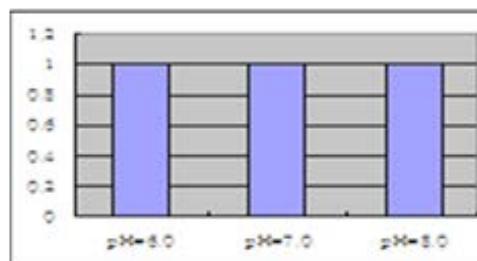
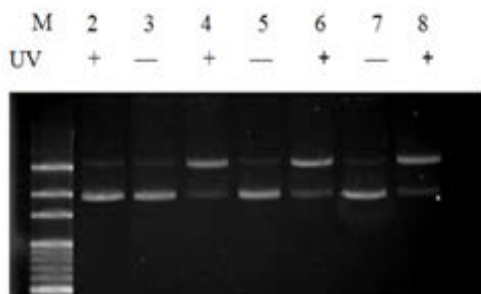


Figure 3.2: DNA cleavage Studies using plasmid pUC19 in presence of 1mM Compound D. Land 1: Marker. Land 2: Control. Land 3: 10mM phosphate buffer, pH=6.0, dark, 1hr. Land 4: 10mM phosphate buffer, pH=6.0, UV=352 nm, 1hr. Land 5: 10mM phosphate buffer, pH=7.0, dark, 1hr. Land 6: 10mM phosphate buffer, pH=7.0, UV=352 nm, 1hr. Land 7: 10mM phosphate buffer, pH=8.0, dark, 1hr. Land 8: 10mM phosphate buffer, pH=8.0, UV=352 nm, 1hr.

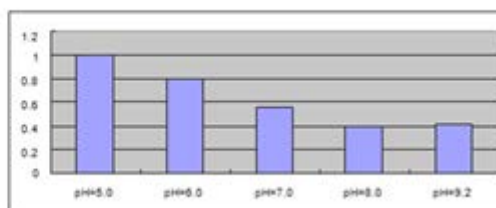
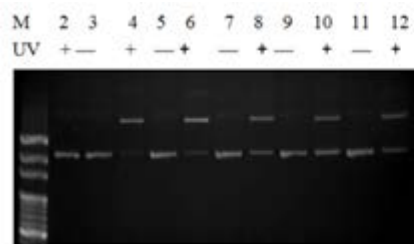


Figure 3.3: DNA cleavage studies using supercoiled plasmid pUC19 in the presence of 1mM Compound D (different pH value). Land 1: Marker. Land 2: Control. Land 3: 10mM phosphate buffer, pH=5.0, dark, 1hr. Land 4: 10mM phosphate buffer, pH=5.0, UV=352 nm, 1hr. Land 5: 10mM phosphate buffer, pH=6.0, dark, 1hr. Land 6: 10mM phosphate buffer, pH=6.0, UV=352 nm, 1hr. Land 7: 10mM phosphate buffer, pH=7.0, dark, 1hr. Land 8: 10mM phosphate buffer, pH=7.0, UV=352 nm, 1hr. Land 9: 10mM phosphate buffer, pH=8.0, dark, 1hr. Land 10: 10mM phosphate buffer, pH=8.0, UV=352 nm, 1hr. Land 11: 10mM phosphate buffer, pH=9.2, dark, 1hr. Land 12: 0mM phosphate buffer, pH=9.2, UV=352 nm, 1hr.

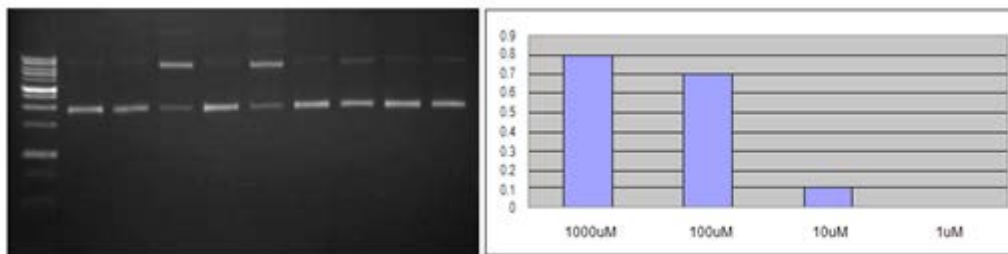


Figure 3.4: DNA cleavage studies using supercoiled plasmid pUC19 in presence of 1 μM~1000 μM concentrations of Compound D, pH=7.0. Land 1: Marker. Land 2: Control. Land 3: 1000 μM compound, dark, 1hr. Land 4: 1000 μM compound, UV=352 nm, 1hr. Land 5: 100 μM compound, dark, 1hr. Land 6: 100 μM compound, UV=352 nm, 1hr. Land 7: 10 μM compound, dark, 1hr. Land 8: 10 μM compound, UV=352 nm, 1hr. Land 9: 1 μM compound, dark, 1hr. Land 10: 1 μM compound, UV=352 nm, 1hr.

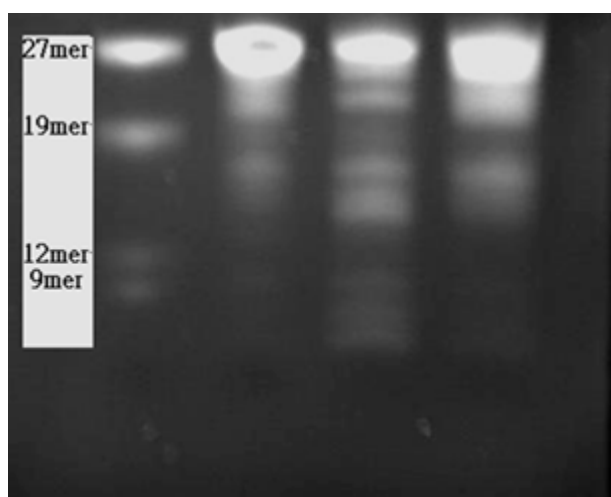


Figure 3.5: The polyacrylamide gel with ethidium bromide staining: Land 1: Marker. Land 2: Control. Land 3: G reaction fragments. Land 4: A+G reaction fragments.

Explore the DNA Cleavage with Site Specificity

Based on above results, we know the compound D has the good cleaving efficiency but the results cannot show if the compound D has the ability of recognize specific nucleobase. Previous literature indicates that the bulged structure is one of the important motifs in DNA recognition. Its unpaired nucleobase are capable of forming complexes with nucleic acid-binding-proteins as well as acting as the bind site for small molecules [37,38]. They were believed to be the intermediates in the fragment shift mutagenesis then lead to some genetic diseases [39,40]. Since DNA stores genetic information, a change in sequences or structures has the potential to induce erroneous gene expression resulting in the information of non-functional proteins.

In order to explore the site-specific DNA cleavage of

the compound D, HIV-27 DNA with bulged structure were treated as DNA template. Dimethyl sulfate (G reaction) and 88% formic acid (A+G reaction) were also used to treat with the HIV-27 DNA to serve as control experiments to help us to check the cleavage site. Here we used different methods to detect the results of experiment. First method is ethidium bromide staining. We added dimethyl sulfate (G reaction) and 88% formic acid (A+G reaction) to HIV-27 DNA that without any labeling respectively, and then added hot piperidine to generate the cleaving patterns. After incubating for 1h, the mixtures were analyzed by gel electrophoresis and stained with ethidium bromide (Figure 3.6). The result displayed two DNA cleavage fragments and indicated the G reaction indeed proceeded. But the results could not identify the cut site of DNA cleavage directly.

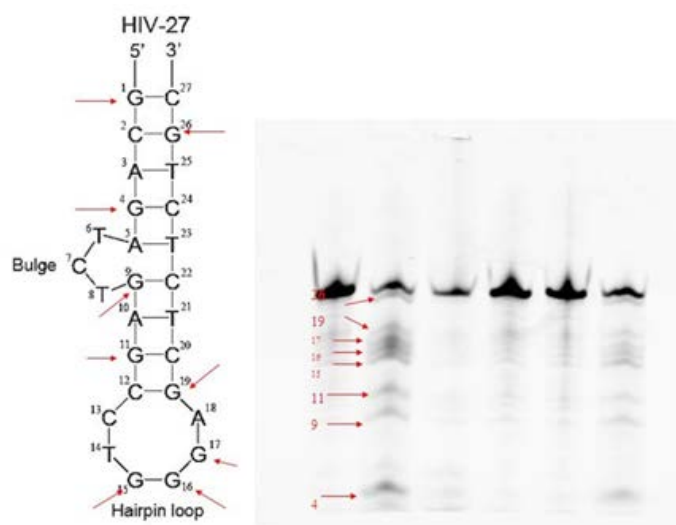


Figure 3.6: HIV-27 DNA with 6 FAM-labelled 5'- terminus detected by typhoon. Land 1: Control. Land 2: G reaction fragments. Land 3: A+G reaction fragments. Land 4: Irradiated with UV light (352-nm) for 1hr. Land 5: 100 μM compound, dark, 1hr. Land 6: 100 μM compound, UV=352-nm, 1hr.

To improve the limitation, we use the chemiluminescence for detection. The HIV-27 DNA was labeled with biotin at 5' end. After analyzing the reaction by gel electrophoresis, the patterns from gel were transferred to the nylon membrane and hybrid with streptavidin-HRP. The biotin and streptavidin have the high affinity. Then, inducing the HRP to produce chemiluminescence and used film to capture the signal. Although it also displayed the cleavage fragment, the single of cleft DNA fragments was too weak to detected.

According to those results, we decided to use the fluorescence for detection. The fluorescence is more sensitive than the two methods describing previously. HIV-27 DNA was labeled with 6 FAM-labelled at 5'- terminus (6 FAM, 6-carboxy-fluorescein). After separating the fragment by gel electrophoresis, we use laser ($\lambda = 488 \text{ nm}$) to excite the 6 FAM and detect the emission at $\lambda = 518 \text{ nm}$ (green light). As the Figure 3-6 shown, it was clearer to see the fragments of G reaction and photoreaction with compound D. The results also indicated that the compound D can recognize guanine residue and cleavage guanine residue directly and proceed the site-specific DNA cleavage. Therefore, compound D might be a candidate for using in anticancer via site-specific DNA cleavage of some important genes. Currently, we are investigating the site at which the DNA was cleaved by compound D.

Conclusion

In this thesis, we apply cantharidin and its derivatives to the pUC19 plasmid or HIV-27 DNA to investigate if they have the function of site-specific DNA cleavage. The previous studies have displayed that cantharidin could cleavage DNA in cell. Hence, scientists tried to design many cantharidin derivatives to cleavage DNA. Base on above, we try to utilize our synthesized cantharidin derivative serving as DNA cleavage agent to cleavage DNA in tumor cells. Our experimental results indicated that compound D possesses the ability to cleavage DNA. In addition, the experiment of site-specific DNA cleavage indicated that compound D can recognize guanine residue and cleavage guanine residue directly. Therefore, cantharidin derivatives could be developed as new photo-induced DNA-cleaving agents via combine with different ligands.

References

1. Woodward RB, Loftfield RB (1941) The Structure of Cantharidin and the Synthesis of Desoxycantharidine. *J Am Chem Soc* 63(11): 3167-3171.
2. Stork G, Tamelen EE, Friedman LJ, Burgstahler AW (1951) Cantharidin. A Stereospecific Total Synthesis. *J Am Chem Soc* 73(9): 4501.
3. Stork G, Tamelen EE, Friedman LJ, Burgstahler AW (1953) A Stereospecific Synthesis of Cantharidin. *J Am Chem Soc* 75(2): 384-392.
4. Dauben WG, Krabbenhoft HO (1976) Organic Reaction at High Pressure Cycloadditions with Furans. *J Am Chem Soc* 98(7): 1992-1993.
5. Dauben WG, Kessel CR, Takemura KH (1980) Simple, Efficient Total Synthesis of Cantharidin via a High-Pressure Diels-Alder Reaction. *J Am Chem Soc* 102(22): 6893-6894.
6. Syntheses and Cytotoxic Effects of Cantharidin-imide, Cantharidin-imine and Relative Analogs, Taipei Medical University, Taipei, 1997.
7. McCluskey A, Ackland SP, Bowyer MC, Baldwin ML, Garner J, et al. (2003) Cantharidin analogues: synthesis and evaluation of growth inhibition in a panel of selected tumour cell lines. *Bioorg Chem* 31(1): 68-79.
8. Wera S, Hemmings BA (1995) Serine/threonine protein phosphatases. *Biochem J* 311(Pt 1): 17-29.
9. Efferth T, Rauh R, Kahl S, Tomicic M, Bozczelt H, et al. (2005) Molecular modes of action of cantharidin in tumor cells. *Biochem Pharmacol* 69(5): 811-818.
10. Tsauer W, Lin JG, Lin PY, Hsu FL, Chiang HC (1997) The effects of cantharidin analogues on xanthine oxidase. *Anticancer Res* 17(3C): 2095-2098.
11. Slupphaug G, Kavli B, Krokan HE (2003) The interacting pathways for prevention and repair of oxidative DNA damage. *Mutat Res* 531(1-2): 231-251.
12. Wang GS (1989) Medical uses of mylabris in ancient China and recent studies. *J Ethnopharmacol* 26(2): 147-162.
13. Tagwireyi D, Ball DE, Loga PJ, Moyo S (2000) Cantharidin poisoning due to "Blister beetle" ingestion. *Toxicol* 38(12): 1865-1869.
14. Pen-Yuan L, Sheng-Jie S, Hsien-Liang S, Hsue-Fen C, Chiung-Chang L, et al. (2000) A Simple Procedure for Preparation of N-Thiazolyl and N-Thiadiazolylcantharidinimides and Evaluation of Their Cytotoxicities against X Human Hepatocellular Carcinoma Cells. *Bioorg Chem* 28(5): 689-700.

- 266-272.
15. Pen-Yuan L, Sheng-Jie S, Lun-Huei L, Hsue-Fen C, Feng-Lin H (2001) Synthesis of Novel N-Pyridylcantharidinimides by Using High Pressure. *J Chin Chem Soc* 48(1): 49-53.
 16. Ferguson LR, Denny WA (1991) The genetic toxicology of acridines. *Mutat Res* 258(2): 123-160.
 17. Jeffrey AM (1985) DNA modification by chemical carcinogens. *Pharmacol Ther* 28(2): 237-272.
 18. Stephens TD, Bunde CJ, Fillmore BJ (2000) Mechanism of action in thalidomide teratogenesis. *Biochem Pharmacol* 59(12): 1489-1499.
 19. Coppel Y, Coulombeau C, Lhomme J, Dheu-Andries ML, Vatton P (1994) Molecular Modelling Study of DNA-Troeger's Bases Interactions. *Biomol Struct Dyn* 12(3): 637-653.
 20. http://en.wikipedia.org/wiki/File:DNA_intercalation2.jpg.
 21. Saenger W (1984) *Principles of Nucleic Acid Structure*. New York: Springer-Verlag, New York.
 22. Watson JD, Crick FH (1953) Molecular structure of nucleic acids; a structure for deoxyribose nucleic acid. *Nature* 171(4356): 737-738.
 23. *Abbreviations and Symbols for Nucleic Acids, Polynucleotides and their Constituents*. IUPAC-IUB Commission on Biochemical Nomenclature (CBN) 1970.
 24. Ghosh A, Bansal M (2003) A glossary of DNA structures from A to Z. *Acta Crystallogr D Biol Crystallogr* 59(4): 620-626.
 25. Yu SSF (2000) *The Chemistry of DNA-Binding and Cleavage Agents*. Chemistry 58.
 26. Pogożelski WK, Tullius D (1998) Oxidative Strand Scission of Nucleic Acids: Routes Initiated by Hydrogen Abstraction from the Sugar Moiety. *Chem Rev* 98(3): 1089-1108.
 27. Berg JM, Tymoczko JL, Stryer L (2002) *Biochemistry*. W.H. Freeman and company, New York.
 28. Alberts B (2002) *Molecular Biology of the Cell*. 4th (Edn.), Garland Science, New York and London.
 29. Burrows CJ, Muller JG (1998) Oxidative Nucleobase Modifications Leading to Strand Scission. *Chem Rev* 98(3): 1109-1152.
 30. Wing R, Drew H, Takano T, Broka C, Tanaka S, et al. (1980) Crystal structure analysis of a complete turn of B-DNA. *Nature* 287(5784): 755-758.
 31. Pabo CO, Sauer RT (1984) Protein-DNA recognition. *Annu Rev Biochem* 53: 293-321.
 32. Helene C (1991) The anti-gene strategy: control of gene expression by triplex-forming-oligonucleotides. *Anticancer Drug Des* 6(6): 569-584.
 33. Mancin F, Scrimin P, Tecilla P, Tonellato U (2005) Artificial metallonucleases. *Chem Commun (Camb)* (20): 2540-2548.
 34. Sitlani A, Long EC, Pyle AM, Barton JK (1992) DNA Photocleavage by phenanthrene diimine complexes of rhodium (III): shape-selective recognition and reaction. *J Am Chem Soc* 114(7): 2303-2312.
 35. Brunner J, Barton JK (2006) Site-specific DNA Photocleavage by rhodium intercalators analyzed by MALDI-TOF mass spectrometry. *J Am Chem Soc* 128(21): 6772-6773.
 36. Chen YJ, Chen PJ, Wang HT, Cheng CC (2004) Specific recognition of DNA bulge structure by matrix-assisted laser desorption/ionization time-of-flight mass spectrometry. *Rapid Commun Mass Spectrom* 18(6): 609-616.
 37. Lilley DM (1995) Kinking of DNA and RNA by base bulges. *Proc Natl Acad Sci U S A* 92(16): 7140-7142.
 38. Wang YH, Bortner CD, Griffith J (1993) RecA binding to bulge- and mismatch-containing DNAs. Certain single base mismatches provide strong signals for RecA binding equal to multiple base bulges. *Biol Chem* 268(23): 17571-17577.
 39. Streisinger G, Owen J (1985) Mechanisms of spontaneous and induced frame shift mutation in bacteriophage T4. *Genetics* 109(4): 633-659.
 40. Kunkel TA (1990) Misalignment-mediated DNA synthesis errors. *Biochemistry* 29(35): 8003-8011.